공학석사 학위논문

Comparative Analysis of Empirical Gas Explosion Models and Blast Resistant Design of PC Panels

가스 폭발 실용모델 및 PC 패널의

방폭설계에 관한 비교분석 연구

2016년 2월

서울대학교 대학원

건축학과

이 수 현

공학석사학위논문

Comparative Analysis of Empirical Gas Explosion Models and Blast Resistant Design of PC Panels

가스 폭발 실용모델 및 PC 패널의 방폭설계에 관한 비교분석 연구

2016년 2월

서울대학교 대학원

건축학과

이수현

Comparative Analysis of Empirical Gas Explosion Models and Blast Resistant Design of PC Panels

지도 교수 강현구

이 논문을 공학석사 학위논문으로 제출함
2016년 2월

서울대학교 대학원
건축학과
이 수 현

이수현의 공학석사 학위논문을 인준함
2016년 2월

위 원 장 _____ (인)

부위원장 _____ (인)

위 원 _____ (인)

Abstract

Comparative Analysis of Empirical Gas Explosion Models and Blast Resistant Design of PC Panels

Ree, Suhyun
Department of Architecture and Architectural Engineering
College of Engineering
Seoul National University

Equipment in onshore plants is installed densely and therefore highly exposed to gas explosion. For protection of life and property, blast resistant design is applied to main buildings, but there are no guidelines for design. Major petroleum companies like BECHTEL or BP plc. make their specifications for blast resistant designs based on TNT equivalent mass. Recently, because gas explosions have various results depending on various external conditions, the TNO multi-energy method or Baker-Strehlow-Tang (BST) methods are mainly used. The conditions are considered in the form of the class or Mach number in the TNO multi-energy or BST method, respectively. The class or Mach number is rarely chosen except by some well-established overseas consultancy companies. This thesis studies which class or Mach number of the TNO multi-energy or the BST method corresponds to the overpressure by existing guidelines, which are based on the TNT equivalency method. The different overpressure, duration, and impulse of three methods are analyzed.

The various design results by these methods are also researched.

Based on the studies, overpressure of the most conservative guideline – the explosion by 1 ton of TNT at a distance of 100 ft. (30.5 m) – has the class number between 6 and 7 or the Mach number between 0.7 and 1.0. When the three methods predict the similar overpressure, the TNT equivalency method provides the shortest duration and smallest impulse. The overpressure by the TNT equivalency method decreases with increasing distance. The higher class or Mach number has shorter duration and larger impulse.

When these methods are applied in blast resistant designs based on this scenario, the TNT equivalency and the TNO multi-energy methods predict the largest and smallest overpressure, respectively. Two response parameters, ductility ratio and support rotation, are used to check design. When blast resistant PC panels are checked, the TNT equivalency, TNO multi-energy and BST methods predict ductility ratio as 10.5, 0.82 and 25.2. Predicted support rotation is 5.1°, 0.4° and 11.5°. Based on these criteria, this wall design only can be passed as evaluated by the TNO multi-energy method. When blast resistant PC panel connections are designed, the ratio of required connection is 3:1:2; TNT equivalency, TNO multi-energy, BST method. These studies show different results when different gas explosion methods are applied on blast resistant designs. Many domestic engineering companies still use TNT equivalent mass for blast resistant designs. As plant design orders of other countries increase, it may be anticipated that research about the TNO multi-energy and BST methods is needed. Because this thesis suggests the relation the TNT equivalency method and the TNO multi-energy or BST methods and shows the different results generated by each, it can help engineers who do blast resistant design with these methods.

Keywords : gas explosion, empirical gas explosion prediction model, equivalent static blast load, blast resistant design, PC panel

Student Number : 2014-20517

Contents

List of Tables

List of Figures

List of Equations

List of Symbols

a	:	depth of compression
a_0	:	sound speed in ambient condition
$A_d A_N$	:	projected surface area for a stud/bolt or group of studs/bolts
A_w	:	effective area of welding
b		leg length of angle
B_H	:	building height
B_L	:	building length
b_n	:	(length of angle)-(hole diameter)-1.6 mm
B_W	:	building width
C	:	coefficient for concentrically loaded weld group
C_1		electrode strength coefficient
C_{crb}	:	cracking coefficient of breakout, 1.0 or 0.8
C_d	:	drag coefficient (1.0 in front wall, -0.4 in side walls and roof)
C_e	:	reduction factor
C_p	:	mean specific heat for liquid propane, 2.41 kJ/kg/K
C_r	:	reflection factor
C_v	:	lag shear coefficient

DIF : dynamic increase factor

E : elastic modulus of material

$E_{comb.}$: combustion energy

e_i : eccentricity of tension or compression

e_v : eccentricity of shear force and construction tolerance

F : flash fraction

F_{du} : dynamic ultimate strength

F_{dy} : dynamic yield strength

F_{EXX} : strength of base meta

F_O : peak force

F_u : ultimate strength of material

F_y : yield strength of material

g : gauge of angle, mm

H_{dn} : designed dynamic horizontal shear force

h_{ef} : effective embedment depth

H_{fuel} : combustion heat of fuel

H_n : designed horizontal shear force

H_{TNT} : combustion heat of TNT

I_W : impulse

I_{avg} : I_{gross}+$I_{cracked}$/2average moment of inertia

$I_{cracked}$: moment of inertia of cracked area

I_{gross} : moment of inertia of gross area

K_{eq} : equivalent stiffness of the member

K_L : load or stiffness transformation factor

K_M : mass transformation factor

k_v : 1.2, coefficient for lag shear coefficient

L : length of member

L_1 : unit element length in blast progressing direction

$L_{propane}$: latent heat for propane = 410 kJ/kg

L_W : blast wave length

M_{eq} : equivalent mass of the member

M_f : Eulerian Mach number

M_w : Lagrangian Mach number

n : number of bolts

N : number of bolts

$N_{bs}C_{bs}$ break out strength coefficient,

N_{dcb} : dynamic nominal concreate break strength

N_{dn} : dynamic designed strength of angl

P_0 : air pressure

P_a : effective side-on overpressure

P_{max} : peak overpressure

P_r : peak reflected pressure

P_{SO} : peak positive overpressure

$\bar{P}_{SO}$: scaled positive overpressure

P_u : applied tension

q_0 : dynamic (blast wind) pressure

R : distance from the center of an origin explosion, ft or m

R_m : maximum resistance of member

S : clearing distance, the smaller of B_H or $B_W/2$

SIF : strength increase factor

t thickness of angle, mm

t_c : clearing time, sec

t_d : positive phase duration

$\bar{t}_d$: scaled positive duration of explosion

t_d^- : negative phase duration

T_{dn} : designed dynamic tensile force

t_n : natural period of structure

U : shock front velocity

V_{cloud} : volume of gas cloud

V_{con} : volume of congested region

V_{dn} : designed dynamic vertical shear force

V_{eff} : min (V_{con},V_{cloud})

V_n : designed vertical shear force

V_u : applied shear force

W : mass of TNT

W_{eff} : actual mass of hydrocarbons in the cloud

W_{fuel} : fuel mass in vapo

W_{TNT} : equivalent mass of TNT

X : distance between bolts in x-direction

Y : distance between bolts in Y-direction

y_e : yield deflection

y_m : maximum deflection

Z, $\bar{R}$: scaled distance

ΔT : gas of temperature

$\Psi_{ed,N}$: edge distance factor

α_0 : yield ratio, 0.03

η : yield factor based on experience (0.03-0.05)

μ : y_m/y_e, ductility demand

θ : support rotation

ρ_b : density of gas after combustion

ρ_u : density of gas before combustion

τ : t_d/t_n, ratio of load duration to natural period

Chapter 1. Introduction

1.1 Background of research

The steady population increase since the Industrial Revolution has resulted in a rapid increase of resource usage. With developed chemical engineering, the petroleum industry, including both onshore and offshore industries, has become one of the largest industries in the world. Unfortunately, gas explosions remain as an all too frequent kind of industrial accident in the petroleum industry. After the Flixborough disaster (1974) and the Piper Alpha disaster (1976), which were typical accidents in the onshore and offshore industries respectively, regulations and guidelines for safety have been suggested and further developed (**Figure 1-1**). In spite of these, however, many gas explosion accidents still occur, causing economic damage and risks to human life. **Tables 1-1** and **1-2** show losses caused by gas explosion in inshore industries.

Figure 1-1 Gas explosion disasters in industry (from left, the Flixborough disaster and the Piper Alpha disaster)

Table 1-1 Top fatalities in onshore incidents from 1970 to 2005 (OGP, 2010)

Fatalities	Number of accidents	Number of gas accidents
>500	3	1
>100	2	1
>10	50	41
Total	55	43 (78%)

Note: This table was made with accidents having occurred in Britain and United States.

Table 1-2 Top costs in onshore incidents from 1970 to 2005 (OGP, 2010)

Cost ($\times 10^6$ USD actual)	Number of accidents	Number of gas accidents
>500	2	2
>90	31	23
Total	33	25 (76%)

Populated areas are also a high-risk area for explosion accidents. The New London Schools explosion (1937) and the Ahyeon-dong gas explosion (1994) showed the horrible consequences that result from gas explosions occuring in cities (**Figure 1-2**). As cities grow larger and larger, and population densities increase, so does the usage of gas in these areas. These factors contribute to a high potential for a gas explosion to occur.

Figure 1-2 Gas explosion disasters in life region (from left, the New London S chools explosion and the Ahyeon-dong gas explosion)

As explained above, the threat of potential gas explosion accidents exists in both industrial and residential sectors. Therefore, blast resistant designs are necessary in order to protect both people's lives as well to reduce property damage from general accidents. With the exception of some countries, however, these designs are not commonly used.

1.2 Objective

Although gas explosions are of considerable concern for both on and offshore industries, the focus here is on onshore industries only as the offshore industry requires considerable expertise. There are various methods to predict the results of gas explosions. These methods are categorized in three different models; the empirical model, the semi-empirical model and computational fluid dynamics (CFD). Onshore industry usually uses the empirical model because it is more economical. Because there is no guideline for determining blast load, some major foreign companies like BECHTEL and BP plc. made and used their own specifications for blast load. These specifications were based on the distance and quantity of TNT (TNT equivalency method). Today, blast load is obtained based on new methods; the TNO multi-energy method or the Baker-Strehlow-Tang (BST) method. These methods predict effects of gas explosions based on class or Mach number, which is determined by various factors. Because estimating class or Mach number requires special knowledge and expertise, only some foreign companies can estimate them accurately. In Korea, most engineers have little or no information about these new methods or how they are different. There are various comparisons of the new methods but no study exists detailing the relationship between the existing guidelines and the new methods. Explaining that relationship can help engineers understand the new methods. For these reasons, this thesis seeks to research the class or Mach number of the existing guidelines and explain differences between those empirical methods. Comparisons of these methods are analyzed in accordance with different results per each method;

gas explosive effects, structural responses and blast resistant connection design. These comparisons can help engineers to understand the new methods and their differences. Additionally, it is expected to guide engineers who want to design blast resistant structures by explaining procedures of blast resistant design.

Chapter 2. Literature Review

2.1 Gas explosion

2.1.1 Definition of explosion

It can be generally said that an explosion is a phenomenon that occurs when energy or pressure is suddenly released. Explosions are marked by a rapid reaction, light, heat, loud noise and so on. Explosions may be classified in a variety of different ways, including: the physical phase of the material's origin, the origin of any explosive material, the origin of the explosion, and finally, of the process of the explosion itself. With regards to the latter of these, explosion processes are generally classified as being either physical or chemical explosions. Additional explosions such as nuclear explosions, electrical explosions, natural explosions such as the eruption of a volcano, or an astronomical explosion like a supernova, are also included in this category (**Figure 2-1**).

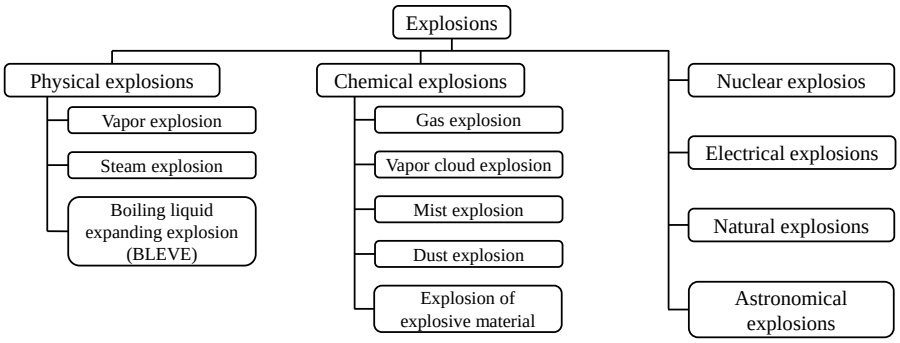

Figure 2-1 Classification of explosions (KASS, 2015) (in Korea)

2.1.2 Characteristics of gas explosion

Gas explosions are caused by the drastic combustion of gas such as natural gas, methane, propane, hydrogen, etc. They are usually caused by vapor cloud premixed with air, with resulting damage being quite large. When the combustion reaction of an explosion is drastic and the speed is lower (or higher) than the speed of sound, it is called a deflagration (or a detonation). The degree of violent combustion determines the result of a gas explosion, and many factors can influence the degree; ignition, geographic conditions like confinement and density of obstacle, reactivity of gas, and so on. There are references explaining the effect of each factor (Bjerketvedt et al., 1997; Casal, 2007; CCPS, 2010).

Accordingly, a gas explosion is described as a typical chemical explosion. Unconfined vapor cloud explosions (UVCE) or vapor cloud explosions (VCE), which are the most powerful disasters occurring in the petroleum industry, are also considered as sorts of gas explosions

2.2 Empirical model

Explosions emit a large amount of energy over a very short period of time. As a result, the blast load cannot be measured by the same method as a wind or seismic load. The blast load is composed of two different blast waves progressing in every direction upon an explosion's release of energy. One of these blast waves is the shock wave, and the other is the pressure wave. Shock waves exert pressure over the air pressure (P_0) without rising time. After a rapid decrease of pressure, the negative pressure phase follows. Pressure waves have rising time to peak pressure. Negative phases also follow a similar path to shock waves. The main parameters for blast waves are the peak side-on positive (or negative) peak overpressure, P_{SO} (or P_{SO}^-), the positive (or negative) phase duration, t_d (or t_d^-), and the corresponding positive (or negative) impulse, I_O (or I_O^-). In addition to these parameters, the peak

reflected pressure, P_r, the peak dynamic pressure, q_0, the shock front velocity, U, and the blast wave length, L_W, are also required for a blast load (ASCE, 2010). These secondary parameters can be determined by the peak overpressure. Because this value varies with different types of explosions, there are various methods to determine the overpressure. In this chapter, a literature review is carried out as to the various research methods predicting the results of gas explosions, and a comparison of these methods is offered.

It is extremely important to prevent gas explosions due to the frequency of gas explosion accidents occur and the large damage they cause in both onshore and offshore industrial accidents. It is not easy to estimate the effect of a gas explosions because of the complex reaction mechanisms and the many variables that may be involved with any particular explosion. Some of these variables include: the reactivity of the fuels involved, confinement, the location and density of obstacles, the complexity of equipment, the shape of a room, etc. Some models have been developed to help simply the procedures involved with predicting a gas explosion's effect. There are three primary gas explosion models, namely, the empirical model, the semi-empirical model, and the computational fluid dynamics (CFD). Each model employs various and distinct methods and the user may choose the appropriate model and method on a case by case basis.

2.2.1 Empirical model

The empirical model depends on the relationship between experimental data and its analysis. The overpressure is calculated with the non-dimensional scaled distance. This varies depending on the distance from the center of the explosion. Each kind of explosion has its own scaled distance equation. In order to determine the scaled distance, the Hopkinson-Cranz scaling law is used in the TNT equivalency method, which is a generally used method for blast resistant design. The scaled distance, Z, is obtained by **Eq. (2-1)**. Sachs' scaling law is also used to obtain the scaled distance, $\bar{R}$, by **Eq. (2-2)**.

$$Z = \frac{R}{W^{1/3}} \tag{2-1}$$

$$\overline{R} = \frac{R}{\left(E_{comb.} / P_0\right)^{1/3}} \tag{2-2}$$

Where,

Z, $\overline{R}$	:	scaled distance
R	:	distance from the center of an origin explosion, m
W	:	mass of TNT, kg
$E_{comb.}$	:	combustion energy, J
P_0	:	air pressure, Pa

The empirical method calculates the results of the explosion in conjunction with data interpolation. Computer programming helps these calculations to proceed simply and quickly. If, however, the scenario being investigated is out of the range of the experimental data, the accuracy of the analysis decreases and the empirical method cannot be applied. The methods widely used in the industrial sector are introduced below.

2.2.2 TNT equivalency method (TNT EM)

The TNT equivalency method is generally used for blast resistant designs based on a crucial assumption; namely, that a gas explosion has similar characteristics to the explosion caused by explosives. This method was first developed by the U.S. Navy and the U.S. Air force first and was originally contained in the US Army Technical Manual TM 5-1300. The US army established correlations between the quantitative of explosives and their resulting damage through a careful analysis of various military experiments. They also found the correlation between TNT equivalency and gas explosions' strength (**Figure 2-2**) after observing the damage caused by a multitude of gas explosion. Consequently, the TNT equivalency method can be used simply by calculating the TNT equivalency corresponding to the

hydrocarbons present. The equivalent mass of TNT is obtained by **Eq. (2-3)**.

$$W_{TNT} = 10\eta W_{HC} \tag{2-3}$$

Where,

W_{TNT}	:	equivalent mass of TNT, kg
η	:	yield factor based on experience (0.03-0.05)
W_{eff}	:	actual mass of hydrocarbons in the cloud, kg

The constant 10 means combustion heat by hydrocarbons is larger than the combustion heat by TNT by roughly ten times (Lea and Ledin, 2002). The TNT equivalency considers only one explosion by total combustion mass, which is a more conservative result than a real gas explosion. In addition, it is challenging to apply TNT equivalency method to a gas explosion because of gas explosions' inherent geometric variables, most notably, obstacle density and location, confinement, etc. Thus, Bjerketvedt et al. (1997) recommended not using the TNT equivalency method for a gas explosion.

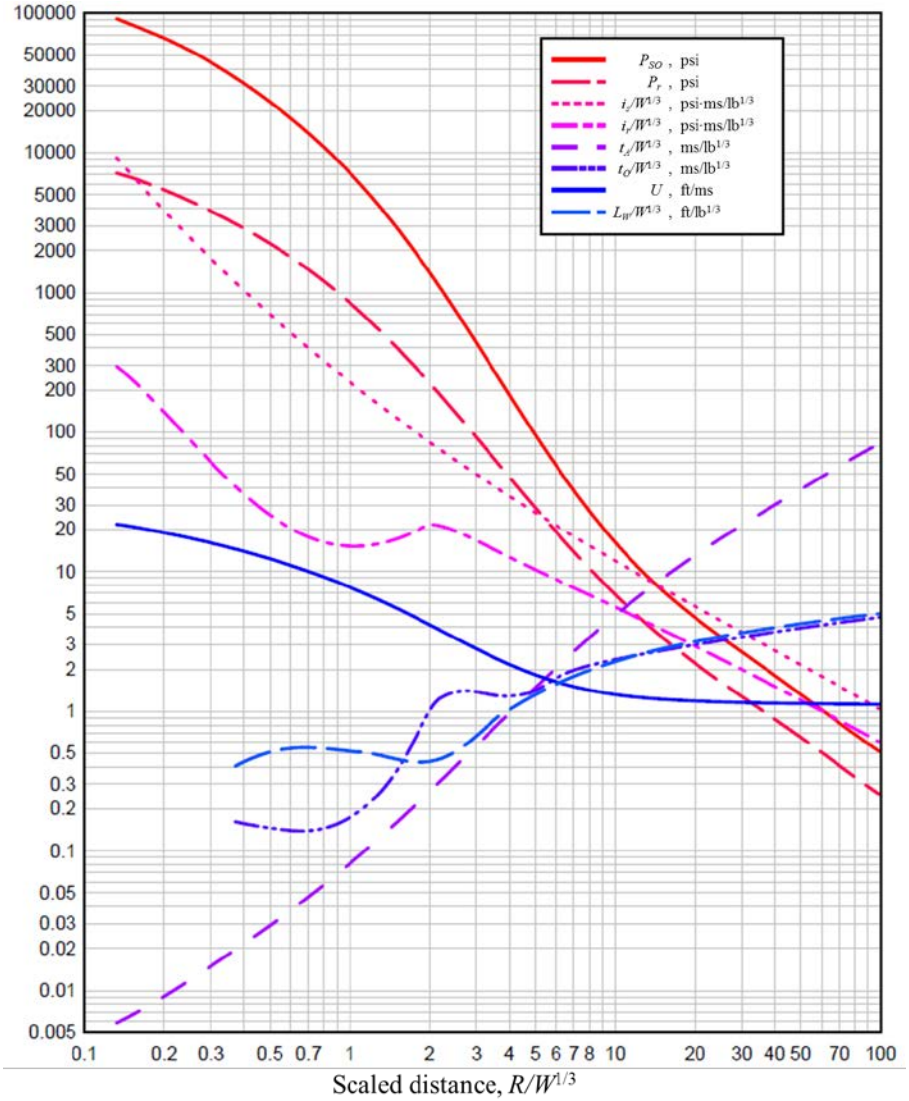

(a) Spherical explosion

P_r : the peak positive normal reflected pressure, psi; P_{SO} : the peak positive incident pressure, psi; $i_r/W^{1/3}$: the scaled unit positive normal reflected impulse, psi·ms/lb$^{1/3}$; $i_s/W^{1/3}$: the scaled unit positive incident impulse, psi·ms/lb$^{1/3}$; $t_A/W^{1/3}$: the scaled time of arrival of positive phase, ms/lb$^{1/3}$; $t_O/W^{1/3}$: the scaled positive duration of positive phase, ms/lb$^{1/3}$; U : the shock front velocity, ft/ms; W : charge weight, lb; $L_w/W^{1/3}$: the scaled wavelength of positive phase, ft/lb$^{1/3}$

(Conversion : 1 ft = 0.3 m; 1 lb = 0.45 kg, 1 psi = 6.89 kPa)

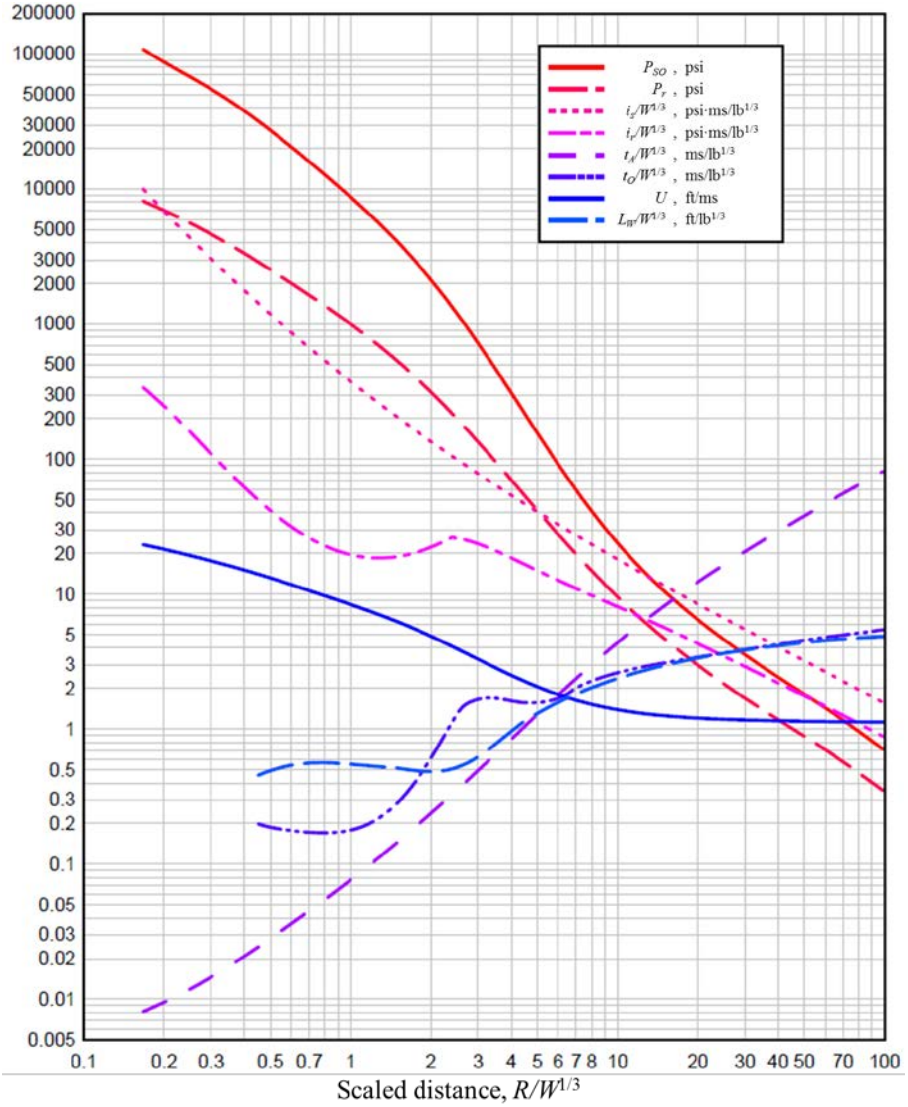

(b) Hemispherical explosion

P_r : the peak positive normal reflected pressure, psi; P_{SO} : the peak positive incident pressure, psi; $i_r/W^{1/3}$: the scaled unit positive normal reflected impulse, psi·ms/lb$^{1/3}$; $i_s/W^{1/3}$: the scaled unit positive incident impulse, psi·ms/lb$^{1/3}$; $t_A/W^{1/3}$: the scaled time of arrival of positive phase, ms/lb$^{1/3}$; $t_O/W^{1/3}$: the scaled positive duration of positive phase, ms/lb$^{1/3}$; U : the shock front velocity, ft/ms; W : charge weight, lb; $L_w/W^{1/3}$: the scaled wavelength of positive phase, ft/lb$^{1/3}$

(Conversion : 1 ft = 0.3 m; 1 lb = 0.45 kg, 1 psi = 6.89 kPa)

Figure 2-2 Results by shapes of blast waves (UFC, 2008)

Harris and Wickens (1989) have suggested a modified TNT equivalency method accounting for various geometric effect based on their experiments. They increased the yield factor to 0.2 and assumed stochiometrically that the hydrocarbon mass would be the same as the gas mass in the highly congested part of a plant. The equivalent TNT is calculated with this modified TNT equivalency method equation, **Eq. (2-4)**.

$$W_{TNT} = 0.16\, V_{eff} \qquad (2\text{-}4)$$

Where,

W_{TNT}	:	equivalent mass of TNT, kg
V_{eff}	:	min (V_{con}, V_{cloud})
V_{con}	:	volume of congested region, m^3
V_{cloud}	:	volume of gas cloud, m^3

As most hydrocarbons have similar combustion heat, 3.5 MJ/m^3, this equation can be applied for most hydrocarbons. The CMR (Hjertager et al, 1981; Hjertager et al., 1982) experimental results for 50 m^3 gas cloud or congested region volume confirmed that the empirical formula suggested by Harris and Wickens predicted the results quite well (Lea and Ledin, 2002). However, in case of a weak gas explosion, which has an overpressure under 1 bar, it tends to overestimate the overpressure, requiring that more accurate measuring methods be used. Other notable drawbacks of the TNT equivalency method are that the general yield factor is necessary and that the charge center is difficult to determine.

2.2.3 TNO multi-energy method (TNO MEM)

Although the TNO method (Wiekema, 1980) and the Multi-energy method (Van den Berg, 1985) were introduced separately, they have more recently become known together as the 'TNO multi-energy method'. One of the reasons for this combination is that the two methods share similar concepts with one important difference, that is, a factor thought to contribute to the overpressure of a gas explosion. According to the TNO method, this factor is a total vapor cloud whereas Multi-energy method assumes that a confined or obstructed part in a vapor cloud affect a result (Lea and Ledin, 2002). In the past, the TNO method and TNT equivalency method were both used to calculate the physical effects of dangerous materials escaping (CPR14E, 1979), but the Multi-energy method has begun to replace the TNO method by Mercx and Van den Berg (1997).

This section mainly focuses on the Multi-energy method, but following recent trends the TNO multi-energy method is noted as (TNO MEM) in what follows. As previously explain, the TNO MEM, suggested by Van den berg (1985), predicts the peak overpressure in different explosion strengths by confinement or obstruction. Obstacles within a gaseous cloud can influence the severity of gas explosions by providing positive feedback on the speed of flame. Turbulence on the surface of obstacles accelerates the flames of an explosion and these accelerated flames create more turbulence. Assuming that turbulence dictates the strength of a blast wave, the TNO MEM defines geographic conditions as a main factor to estimate the potential energy of gas explosions – obstructed and confined. In addition to different ignition sources in a vapor cloud, it reflects effects of positive overpressures and positive duration phases considering sub-explosions having different strength. The procedure estimating the strength of explosions with TNO MEM is as follows :

(1) Determine obstructed and/or unobstructed regions.

(2) Predict a class number or source strength of each region.

(3) Estimate the radius of a vapor cloud.

(4) Determine the scaled distance, positive scaled overpressure and scaled duration phase: blast parameters

(5) Calculate the positive overpressure, positive duration and positive impulse: real parameters

The scaled distance of blast parameters, which are used to estimate the result of a gas explosion, is calculated by Sach's law, **Eq. (2-2)**. Since hydrocarbons have a similar combustion heat (3.5 MJ/m^3), they also have a similar combustion energy and this energy is dependent on the total volume of the vapor cloud. The combustion energy of a vapor cloud is calculated by **Eq. (2-5)**.

$$E_{comb.} \approx 3.5 V_{cloud} \qquad (2\text{-}5)$$

Where,

$E_{comb.}$: combustion energy of gas cloud, J
V_{cloud} : volume of gas cloud, m^3

The blast parameters, positive scaled overpressure, positive scaled dynamic pressure and scaled duration phase, are determined through graphs. The TNO MEM provides the graphs: the scaled parameters versus the scaled distance. After the scaled distance is determined, the scaled distance, positive scaled overpressure and scaled duration phase can be calculated in conjunction with **Figure 2-3**. These values are dependent on the class number. The overpressure, duration of positive phase and impulse are all calculated by **Eqs. (2-6), (2-7)** and **(2-8)**, respectively.

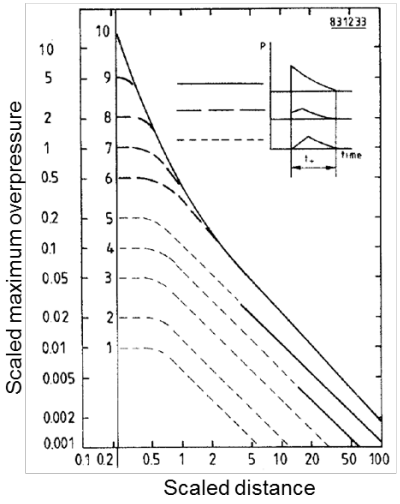

(a) Scaled overpressure

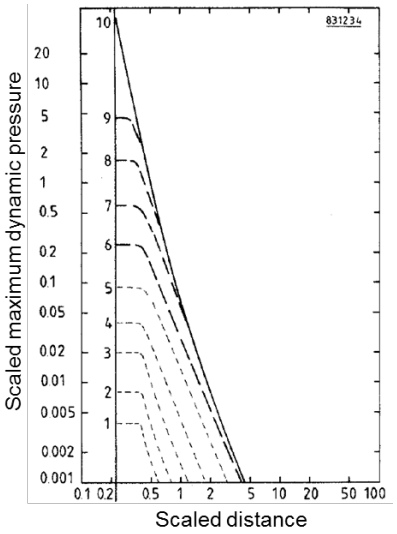

(b) Scaled dynamic pressure

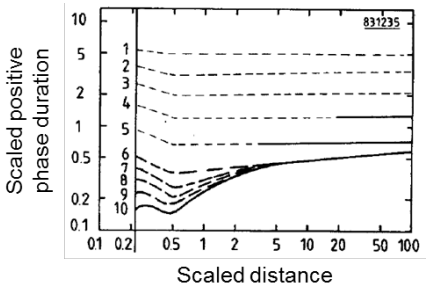

(c) Scaled duration

Figure 2-3 Blast parameters by TNO MEM (Van den Berg, 1985)

$$P_{SO} = \overline{P_{SO}} \times P_0 \qquad (2\text{-}6)$$

Where,

P_{SO} : positive overpressure, Pa
$\overline{P_{SO}}$: scaled positive overpressure
P_a : air pressure, Pa

$$t_d = \overline{t_d} \times \left(\frac{E_{comb.}}{P_0} \right)^{1/3} \times \frac{1}{a_0} \qquad (2\text{-}7)$$

Where,

t_d : positive duration of explosion, sec
$\overline{t_d}$: scaled positive duration of explosion
a_0 : sound speed in ambient condition, m/s

$$I_W = \frac{P_{SO} \times t_d}{2} \qquad (2\text{-}8)$$

The class number indicates the initial strength of a gas explosion. The stronger the strength an explosion has, the higher number it is assigned, and any explosion with the class number 10 is defined as a detonation. The class number is altered by a variety of variables such as the reactivity of the fuel, the presence of confined or obstacles, etc. Some researchers have offered guidance for choosing the class numbers of a gas explosion. Kinsella (1993), for example, has offered a table considering ignition energy, obstacle density, and confinement (**Table 2-1**). Similarly, Roberts and Crowley (2004) considered the dimension of an explosion, reactivity, and obstacle density (**Table 2-2**).

These tables only define the range of class numbers and not a certain value. The user must make a final decision when it comes to choosing the appropriate class number, which places a minor constraint on objectivity. The GAME (Eggen, 1998) and GAMES projects (Mercx et al., 1998) were examples of an attempt to resolve this insufficiency.

Table 2-1 Guidelines by Kinsella (1993)

Ignition energy		Obstacle density			Confinement		Class number
Low	High	No	Low	High	No	Existing	
	×			×		×	7 – 10
	×			×	×		7 – 10
×				×		×	5 – 7
	×		×			×	5 – 7
	×		×		×		4 – 6
	×	×				×	4 – 6
×				×	×		4 – 5
	×	×			×		4 – 5
×			×			×	3 – 5
×			×		×		2 – 3
×				×		×	1 – 2
×				×	×		1

Table 2-2 Guidelines by Roberts and Crowley (2004)

Types of flame expansion	Mixture reactivity	Choice of class number		
		Obstacle density		
		High	Medium	Low
1D	High	10	10	10
	Medium	9 – 10	9	7 – 8
	Low	9 – 10	7 – 8	4 – 5
2D	High	9	7 – 8	6
	Medium	7 – 8	6 – 7	2 – 3
	Low	6	5 – 6	1 – 2
3D	High	6	3	1
	Medium	3 – 4	2	1
	Low	3	2	1

2.2.4 Baker-Strehlow-Tang (BST) method

The BST method suggested and developed by Baker et al. (1996) is described using overpressures and impulses with energy-scaled distance. Baker and other researchers carried out a literature review to determine the flame speed of an explosion according to the Mach number. The Baker and Strehelow method (BS method), which is the basis of all three BST methods, allows users to choose one method among three: 1) The Baker-Strehelow (BS); 2) The Baker-Strehlow-Tang 1 (BST 1), using new sets of curves (Tang et al., 1999; and 3) The Baker-Strehlow-Tang 2 (BST 2), using the new matrix (Pierorazio et al., 2004). Each method uses different matrixes or different curves. For example, the BS method uses the matrix and curves initially suggested (Baker et al., 1996; **Figure 2-4**; **Table 2-3**). The BST1 method uses new curves (Tang and Baker, 1999; **Figure 2-5**) and the BST2 method uses new matrixes and curves (Pierorazio et al., 2004; **Table 2-4**).

The maximum flame speed is marked with the Mach number, which can be changed according to sources, confinement, obstacle density and so on. The Mach number is used to calculate positive overpressures and positive impulses with two sets of curves. This is done in the same way that the TNO MEM was adopted to determine the overpressure. The positive impulse is obtained by **Eq. (2-9)**. If the Mach number is greater than 0.25, the equation suggested by the BST1 method can be used to calculate the impulse. The BST method can be used easily, gives results quickly, and considers geometric conditions and multi-ignition points, allowing for conservative results.

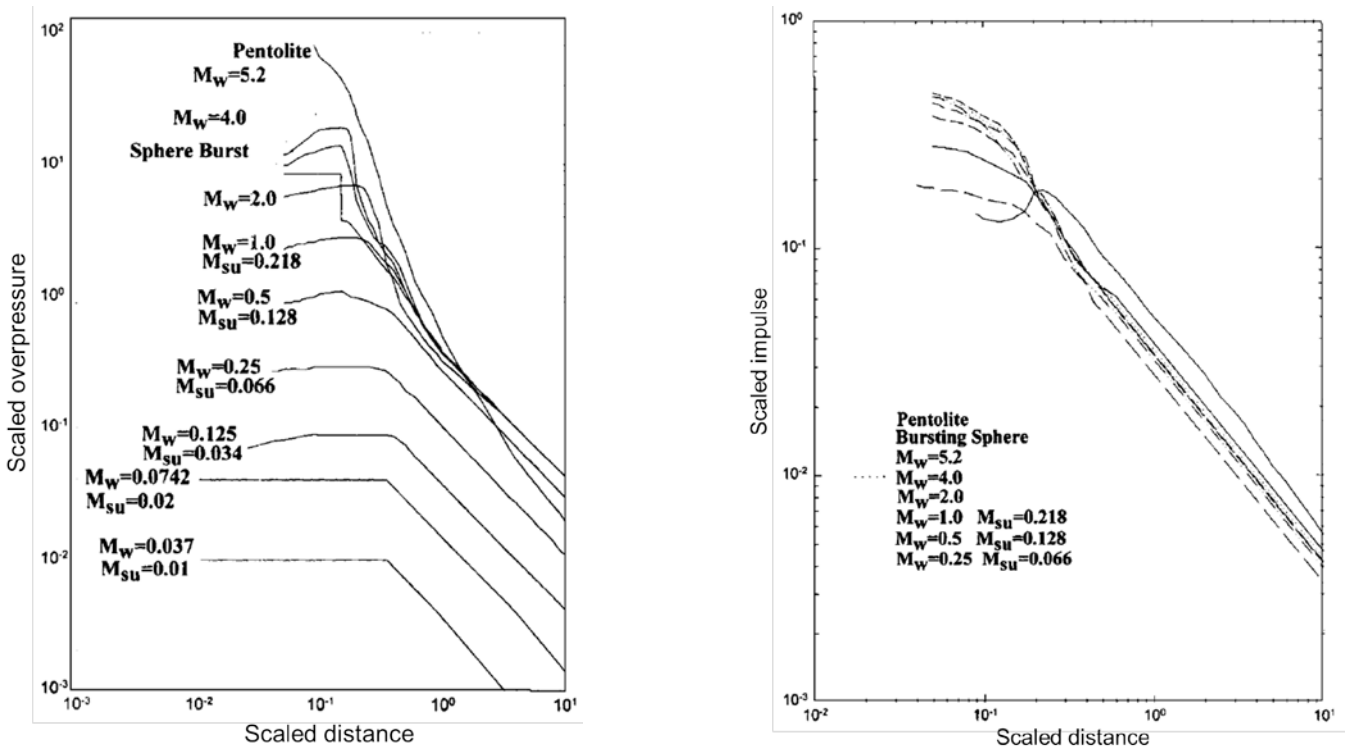

(a) Scaled overpressure

(b) Scaled impulse

Figure 2-4 Baker et al. curves(1996)

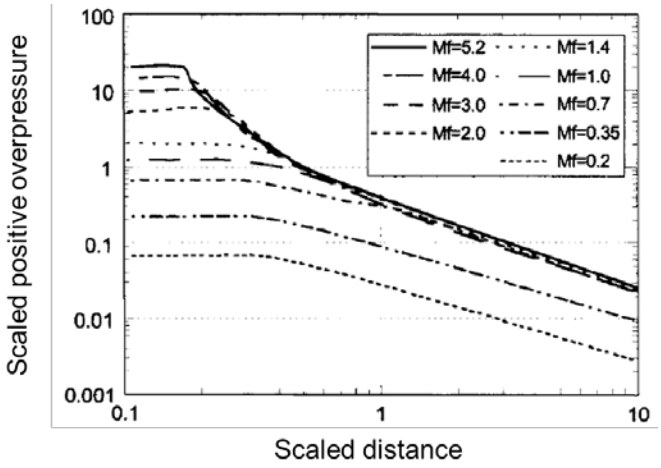

(a) Scaled overpressure

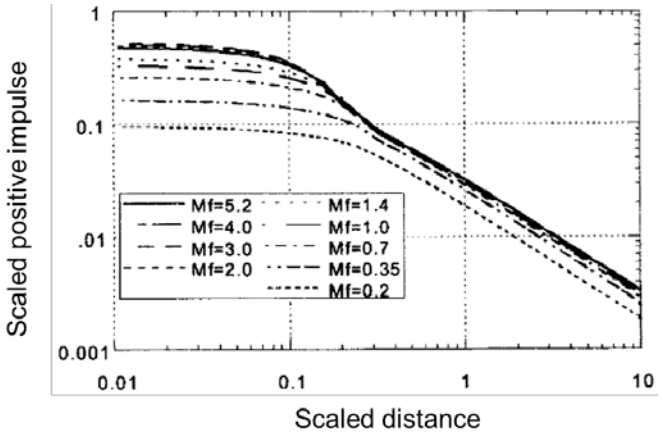

(b) Scaled impulse

Figure 2-5 Tang and Baker curves (1999)

$$I_W = \overline{I_W} \times \left(\frac{E_{comb.}}{P_0} \right)^{1/3} \times \frac{P_0}{a_0} \qquad (2\text{-}9)$$

There are two essentially usable matrixes for choosing the Mach number: the Baker et al. matrix(1994) and the Pierorazio et al. matrix (2004; **Table 2-4**). These two matrixes determine the Mach number by considering the correlations within congestion (obstacle density), fuel reactivity, and flame expansion (confinement).

The Baker et al. matrix (1994) was based on a literature review of experiments involving flame speed. The obstacle influence is defined in relation to different kinds of obstacles, VBR (Volume Blockage Ratio) and Pitch. According to the categories of the TNO MEM, the fuel-reactivity of gas is classified as L (Low reactivity), M (Medium reactivity), or H (High reactivity). The final category of classification is the confinement: flame expansion. There are three kinds of categories based on the manner with which a flame spreads, namely: 1D flame expansion, 2D flame expansion, and 3D flame expansion, spherical of hemispherical flame.

Table 2-3 Baker et al. matrix (1994)

Types of flame expansion	Mixture reactivity	Choice of Mach number, M_w		
		Obstacle density		
		High	Medium	Low
1D (planar flame)	High	5.2	5.2	5.2
	Medium	2.265	1.765	1.029
	Low	2.265	1.029	0.294
2D (cylindrical flame)	High	1.765	1.029	0.588
	Medium	1.235	0.662	0.118
	Low	0.662	0.471	0.079
3D (spherical or hemispherical flame)	High	0.588	0.153	0.071
	Medium	0.206	0.100	0.037
	Low	0.147	0.100	0.037

The Pierorazio et al. matrix (2004) is based on experiments conducted on a medium scale. The congestion region and obstacles are designed as modular sections of cubes with 1.8 m sides and a circular tube. Researches about the

obstacle configuration were conducted for leveling the congestion. The number of tubes and the percentage of VBR divided congestion categories; low, medium, and high. Sixteen tubes, 49 tubes, 65 tubes were used to express the low congestion (VBR is from 0% to 1.5%), medium congestion (VBR is from 1.5% to 4.35%) and high congestion (VBR is from 4.3% to 5.7%), respectively. With regards to the fuel reactivity, methane-air mixture, and propane-air mixture, and ethylene-air mixture were used as low, medium and high reactivity gases, respectively. This matrix follows the reactivity category of the BS matrix. In the Pierorazio et al. matrix, the 1D flame expansion was eliminated because it hardly occurs in real industrial field. The 2.5D flame expansion was added instead, for environmental conditions blocked with fragile panels or solid confining plane. The 2D and 3D flame expansions were remained.

Table 2-4 Pierorazio et al. matrix (2004)

Types of flame expansion	Mixture reactivity	Choice of Mach number, M_w		
		Obstacle density		
		High	Medium	Low
2D (cylindrical flame)	High	DDT	DDT	0.59
	Medium	1.6	0,66	0,47
	Low	0.66	0.47	0.079
2.5D	High	DDT	DDT	0.47
	Medium	1.0	0.55	0.29
	Low	0.50	0.35	0.053
3D (spherical or hemispherical flame)	High	DDT	DDT	0.36
	Medium	0.50	0.44	0.11
	Low	0.34	0.23	0.026

After the Mach number is determined in accordance with the matrix referenced previously, the positive overpressures and positive impulses are calculated with sets of curves. The two sets of curves available in the BST method are the following: 1) The Baker et al. curves (**Figure 2-4**), with a M_w

function, Lagrangian Mach number; and 2) The Tang and Baker curves (**Figure 2-5**), with a M_f function, Eulerian Mach number. The second sets of curves are employed more frequently of late. The first curves use thermal velocity in Lagrangian coordinates, and the other curve uses flame velocity in Eulerian coordinates, measured by a fixed observer. Tang and Baker (1999) suggested the second curves to prevent misuse of the Mach number. The M_w and M_f has the same value in the supersonic region, but below the speed of sound, M_w and M_f followed **Eq. (2-10)**.

$$M_f = M_w \times \left(\rho_u / \rho_b\right)^{1/3} \tag{2-10}$$

Where,

M_w : Lagrangian Mach number
M_f : Eulerian Mach number
ρ_u : density of gas before combustion
ρ_b : density of gas after combustion

It should be noted that the above equation cannot be used when the Mach number is unity. In that case, **Eq. (2-11)** is instead used to calculate the peak overpressure.

$$\frac{\left(P_{max} - P_a\right)}{P_a} = 2.4 \times \frac{M_f^2}{\left(1 + M_f\right)} \tag{2-11}$$

Where,

P_{max} : peak overpressure, Pa

Today the Tang and Baker curves are most frequently used although each method has its own calculation process for positive overpressure and positive impulse. In the BS method, after determining M_w, the overpressure and impulse may be read off. In the BST 1 and the BST 2 methods, after determining M_w for proper M_f, one can follow the same procedure outlined in the BS method.

2.2.5 Congestion Assessment Method (CAM)

The Congestion Assessment Method (CAM) was developed by Cates and Samuels (1991) while working at Thornton Research in Canada. This method was subsequently implemented by Puttock (1995, 1999). Cates and Samuels (1991) designed their decision tree procedure as an introductory means of guessing source pressures. This method takes into account the layout of a particular plant, including confinement, congestment and the kind of fuel in question. Although it estimates the pressure precisely, the calculated result is conservative. This method requires three steps:

First, estimate the congested region allotting the reference pressure, Pref. The reference pressure is the peak overpressure by a propane gas vapor detonation.

Then, multiply the reference pressure from the first step by the fuel factor based on the type of fuel involved.

Finally, calculate the pressure via the distance from the ignition point. Cates and Samuels (1991) followed the decay law, which is inversely proportional to the distance, and Puttock (1995) developed an in-detail computational pressure decay curve based on the experimental data.

Puttock (1999, 2000b) developed his own method, which included the experimental results according to size first published by Mercx (1993). Mercx's experiments, which were a part of MERGE (Modeling and Experimental Research into Gas Explosion) project, consisted of small, medium and large scaled experiments.

Developing CAM2, Puttock (1999, 2000) focused primarily on partially congested regions; for example, 1) a non-symmetric plant; 2) a plant with one way being longer than the other two ways; and 3) regions having smaller gas vapor than congested parts, and problems concerning objects with acute edges, The congestion assessment method has been recognized as one of the most advanced empirical methods available but it should also be noted that this method is only applicable with new scenarios and not with revised models.

First of all, the user evaluates the congestment and confinement in a particular plant. The evaluation is limited to geometric conditions and most plants already have the complicated equipment installed. Although there are guidelines for evaluating the congestment and confinement of a plant, two separate people assessing a plant individually may arrive at two different plant evaluations. This can produce considerably different overpressures in a plant.

The CAM is easy to use and requires little time. It has been employed in many experiments and can approach a reasonable peak overpressure when the extreme index has an infinite value. In addition, a plant having a non-symmetric congested region or narrow and long shape can be assessed using the CAM method. On the other hand, however, it can only provide approximate descriptions of geometrical conditions, and moreover, it lacks the distinctive features required for unique congestment or confinement.

2.3 Other models

2.3.1 Phenomenological model

Phenomenological models make idealized systems such as a single ventilating chamber involving a large grid generating turbulence, rather than creating real scenarios. It is extremely useful when dealing with unique geographic conditions such as those found in offshore industry modules, but less applicable to more complex conditions. In these models the blast mechanic is expressed either experimentally or theoretically. The run time of phenomenological models take just a few seconds. The blast evaluation is based on the scaled distance in terms of an analytical approach to consider the effects of shock waves. Phenomenological models lay between empirical models and the computational fluid dynamics (CFD) in terms of their complexity. The CFD models have in common about some of the mechanics of phenomenological models but they tend to be suited to more complex or arbitrary conditions. Both of these models are used to analyze various scenarios or to choose the special conditions researched within CFD codes. The SCOPE (Shell Code for Overpressure Prediction in gas Explosion) developed at Shell's Thornton Research Center and the CLICHE (Confined LInked CHamber Explosion) developed by Advantica Technologies Ltd. are examples of software commonly used in phenomenological models.

2.3.2 Computational fluid dynamics (CFD)

The Computational fluid dynamics (CFD) solves the Navie-Stroker equation based on the movement of fluid. This model is good for complex geometric conditions like a city environment or buildings with crowded interiors. Eulerian computational methods using finite difference solver like SHAMRC, ANSYS AUTODYN and Air3d. Recently, it has been developed fast and with relatively high accuracy can explain a real scenario without frustrated simplification. However, there are still problems creating a viable combustion

model that accurately expresses flow field turbulence to correctly simulate flame velocity and the flame acceleration process. A number of studies have been conducted to solve this trouble and the CFD code has been subsequently modified. In this code, the air is defined as an ideal gas, and detonation is modeled using proper explosive material state equations. However, the accuracy of CFD simulation is still limited to the numerical calculations and basic physical lower models. Thus, experimental checks are still necessary because models explaining positive feedback of turbulent combustion are highly dependent on an experimental constant. Therefore, the computational code for detailed VCE modeling should be confined to problems proved through experiments. A high level of expertise is required to do so because many variables such as grid and time resolution have a great influence on the results. These kinds of simulations take a long time to construct and run, which is an important consideration in case many scenarios are required (Tang and Baker, 1999).

2.4 Blast load by explosion

2.4.1 Parameters

Methods are searched which are used to determine the overpressure caused by gas explosions above. From here, the procedures for determining blast loads are explained in detail. When an explosion occurs, the volume of gas increases rapidly and fluid is compressed. Compressed fluid progresses in all directions and influence environments as a wave, so called the blast wave (**Figure 2-6**). When the blast wave peaks suddenly without rising time, it is usually called as the shock wave.

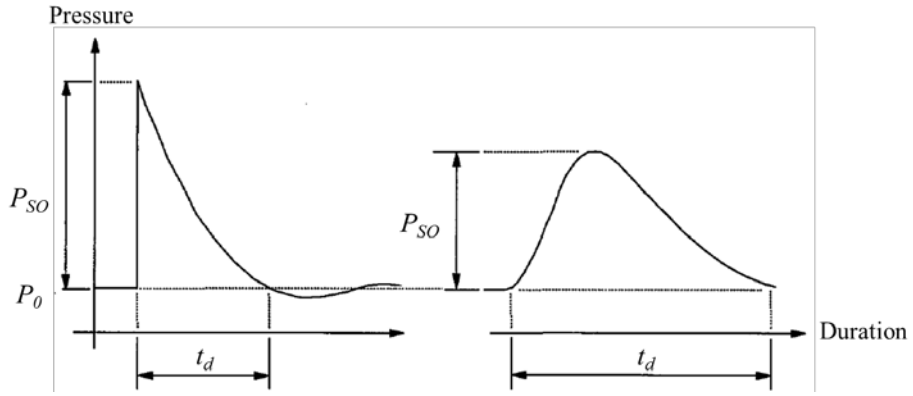

(a) Shock wave (b) Pressure wave

Figure 2-6 Blast waves (ASCE, 2010)

For blast resistant design, the overpressure is used to calculate the peak reflected pressure, P_r, the peak dynamic pressure, q_0, the shock front velocity, U, and the blast wave length, L_W.

2.4.1.1 Peak overpressure (P_{SO})

Blast waves load buildings as overpressure and the peak overpressure of a gas explosion is dealt as static load (Nasr and Coner, 2014). The peak overpressure, P_{SO}, is a primary value for blast resistant design with the duration, t_d. These values are given by an owner. TNT equivalency method is

generally used to determine the peak overpressure, but as explained previously, the peak overpressure caused by gas explosions should be predicted by other methods; namely, TNO multi-energy method or Baker-Strehlow-Tang method.

2.4.1.2 Peak reflected pressure (P_r)

In an unconfined field, the blast waves go forward and are partially reflected by the ground. These reflected blast pressure waves are superposed by any following blast waves. The superposition makes buildings experience a larger overpressure than a peak overpressure. This larger overpressure is the peak reflected pressure, P_r, which is calculated by multiplying the reflection coefficient, C_r, and the peak overpressure. The reflection coefficient is dependent on the peak overpressure, the type of blast waves, the angle, α, between the surface and the front of the blast waves (**Figure 2-7**). The reflection coefficient could be obtained by **Eq. (2-12)** when the peak overpressure is smaller than 138 kPa and the angle, α, is zero.

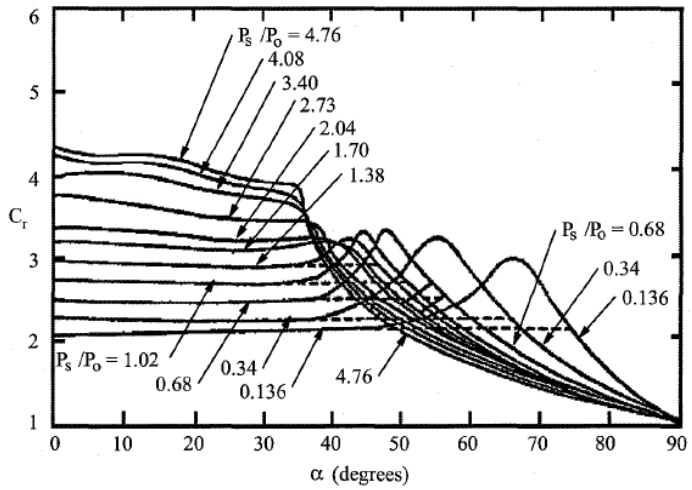

(a) Shock wave

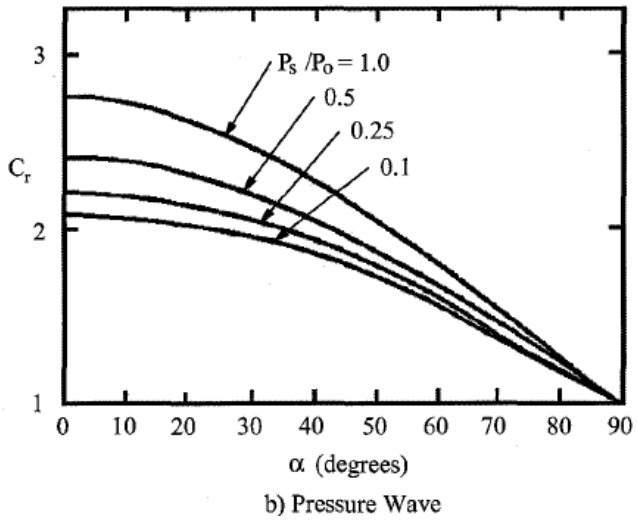

(b) Pressure wave

Figure 2-7 Reflected coefficient of shock and pressure wave

$$C_r = P_r / P_{SO} \approx 2 + 0.0073 P_{SO} \qquad (2\text{-}12)$$

2.4.1.3 Dynamic (blast wind) pressure (q_0)

With progressing blast waves, gas moves and generates the dynamic (blast wind) pressure, q_0. It depends on the peak overpressure. The dynamic pressure is obtained by **Eq. (2-13)**.

$$q_0 = 2.5P_{SO}{}^2 / \left(7P_a + P_{SO}\right) \approx 0.0032P_{SO}{}^2 \qquad (2\text{-}13)$$

When the dynamic pressure is applied in structures, different parts have different dynamic pressure, multiplying the drag coefficient, C_d, and the dynamic pressure. In a rectangular building, the front wall, facing the origin of explosion, has the drag coefficient, 1.0. The other parts like side walls, the rare wall and the roof, has -0.4.

2.4.1.4 Shock front velocity (U)

In a confined space, the velocity of blast waves progressing through a medium is the same or even higher than the velocity of sound. UFC 3-340-02 (2008) provides graphs for the front velocity of shock waves in accordance with the scaled distance. Pressure waves are rarely similar to shock waves, but importantly for design, pressure waves are expected to move at the same velocity of shock waves for conservative results. The shock front velocity is calculated with the peak overpressure, as shown in **Eq. (2-14)**.

$$U \approx 345\left(1 + 0.0083P_{SO}\right)^{0.5} \text{ (m/s)} \qquad (2\text{-}14)$$

2.4.1.5 Blast wave length (L_W)

The peak overpressure is at its highest in the front and decreases gradually in accordance with the distance, L_W. The blast wave length is calculated as in **Eq. (2-15)**.

$$L_W \approx U \times t_d \qquad (2\text{-}15)$$

2.4.2 Blast load applied on members

As the blast waves caused by a gas explosion strike a building, they undergo both peak overpressure and drag force. The original interaction between the building and the blast waves involved quite a complex mechanism (**Figure 2-8**). In blast resistant designs, the explosion is assumed to load uniformly on each wall (**Figure 2-9**). Blast waves progress from left to right as seen in **Figure 2-9**, but the direction of the blast waves could change depending on the explosive origin. The distance and direction of the explosive origin can potentially result in various combinations of blast effects. Therefore, design engineers must determine the blast load on each individual part with the peak overpressure and the duration given by owners.

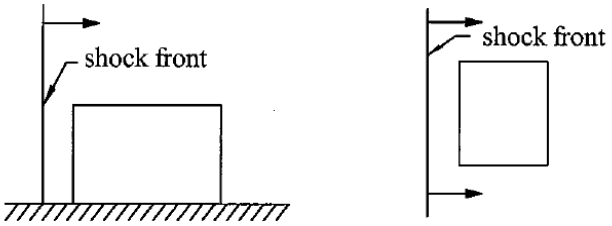

(a) Shocks front progressing to the building

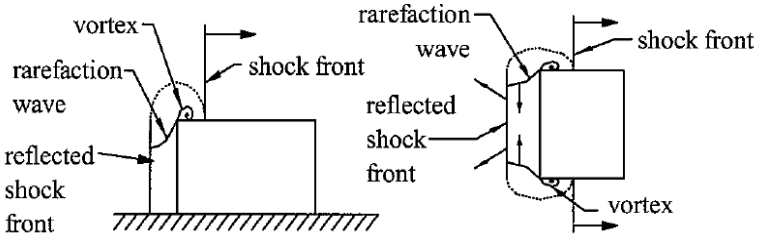

(b) Shock waves reflected in the front and diffracting over structure

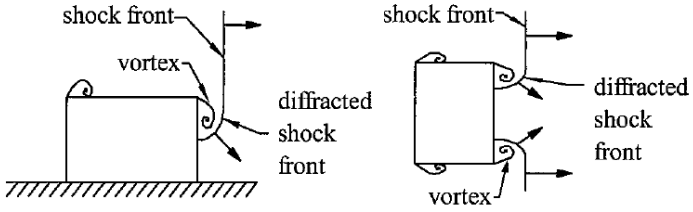

(c) Continuous diffraction on rear wall

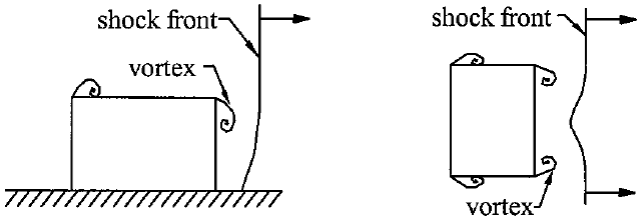

(d) Completed diffraction and shock waves already passing

Figure 2-8 Schematic interaction between shock wave and rectangular building (ASCE, 2010)

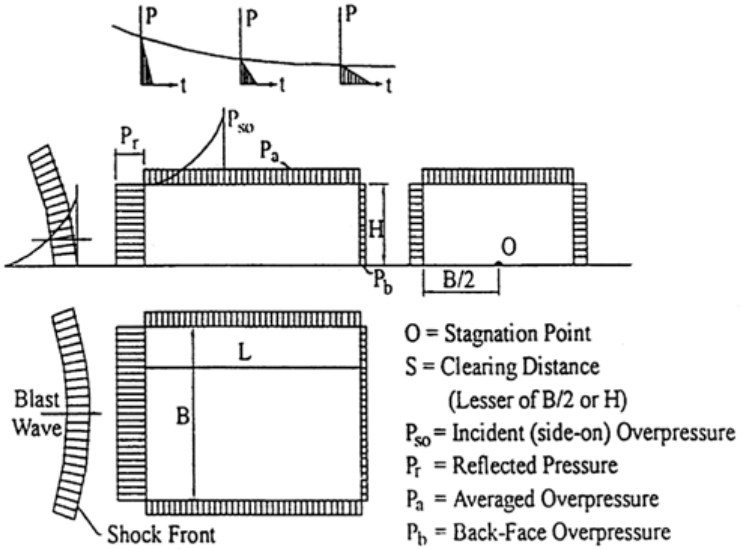

Figure 2-9 Schematic interaction between shock wave and rectangular building (ASCE, 2010)

2.4.2.1 Front wall

The front wall, which faces the origin of an explosion, is loaded by the explosion's reflected pressure. As previously described, the reflected pressure is dependent on the angle between the surface and the wave front, α, as well as the rise-time, t_r. Without any specifications with regards to design, the angle, α, and rise-time are set as zero. The blast load applied on front walls decreases rapidly following the reflected pressure. After clearing time, t_c, the blast load decreases slower following the stagnation pressure, P_S. The stagnation pressure and the clearing time are calculated following **Eqs. (2-16)** and **(2-17)**. A bilinear pressure-time graph by the reflected and stagnation pressure is simplified to the equivalent triangular graph, which has the same impulse, I_W (**Figure 2-10**). The duration by the equivalent triangle is calculated using impulse, I_W, following **Eqs. (2-18)** and **(2-19)**.

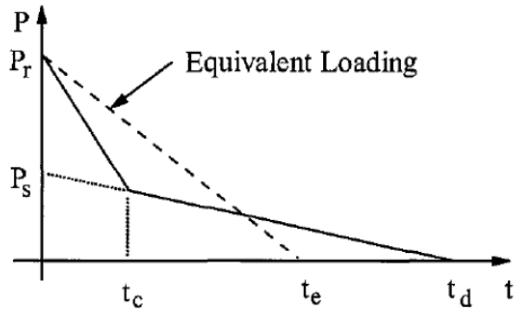

Figure 2-10 Pressure-time graph for front wall (ASCE, 2010)

$$P_s = P_{so} + C_d q_0 \tag{2-16}$$

$$t_c = 3S/U < t_d \tag{2-17}$$

$$I_W = 0.5(P_r - P_S)t_c + 0.5P_S t_d \tag{2-18}$$

$$t_e = 2I_W/P_r = (t_d - t_c)P_S/P_r + t_c \tag{2-19}$$

2.4.2.2 Side wall

The side-wall generally experiences lower pressure than the front wall. The reflected pressure decreases and the blast waves weaken according to the distance. The side-on overpressure doesn't act uniformly in blast waves as they move decreasingly following the longitudinal direction of surrounding elements. In design, the reduction factor, C_e, is used to represent this. The reduction factor, C_e, is dependent on the ratio of the length of the blast wave, L_W, and the unit element length in the blast progressing direction, L_1 (**Figure 2-11**). The effective side-on overpressure, P_a, is calculated by **Eq. (2-20)** (**Figure 2-12**). Side walls have rising time as blast waves travel the elements. The total duration of side wall loading is equal to the rise time and the duration of blast. This is described in **Eq. (2-21)**.

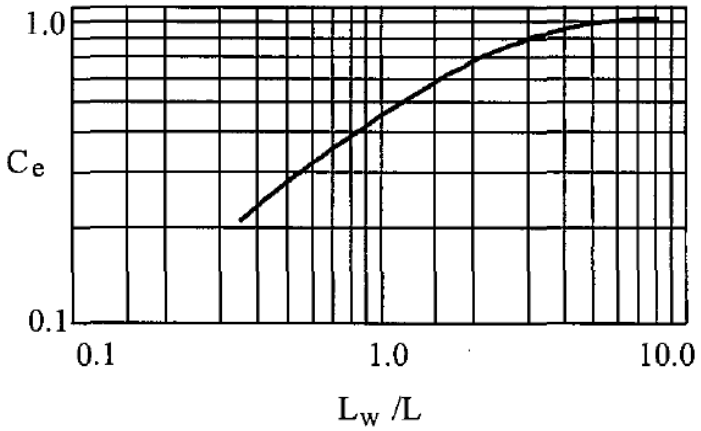

Figure 2-11 Reduction factor (ASCE, 2010)

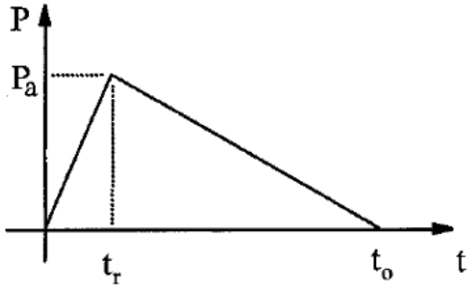

Figure 2-12 Pressure-time graph for side wall and roof (ASCE, 2010)

$$P_a = C_e P_{SO} + C_d q_0 \tag{2-20}$$

$$t_0 = t_r + t_d, \quad t_r = L_1/U \tag{2-21}$$

2.4.2.3 Roof

On roofs with which there is a slope below ten degrees, blast waves are assumed to be passing parallel with the roof without any reflecting. The roof is applied with the combined load, side-on overpressure and dynamic wind pressure as side walls. The effective side-on overpressure loaded on the roof is calculated using the same equation as is used for side walls.

2.4.2.4 Rear wall

The load on the rear wall has the opposite direction as the front wall load. For a conservative design, the load on the rear walls is ignored except evaluating net overall frame load acting on frame. The rear wall has a similar load shape to the side wall or roof; and there is a delayed emergence time as blast waves pass through the building. The ground reflection effect and the possibility of spillover to side and rear walls make it difficult to determine rise-time and duration accurately. The TNO Green book (1992) sets rise-time as four times the travel time of a blast wave on a clearing distance referring to ASCE Manual 42. UFC3-340-02 (2008) sets rise-time as travel time of blast waves on a clearing distance (**Figure 2-13**).

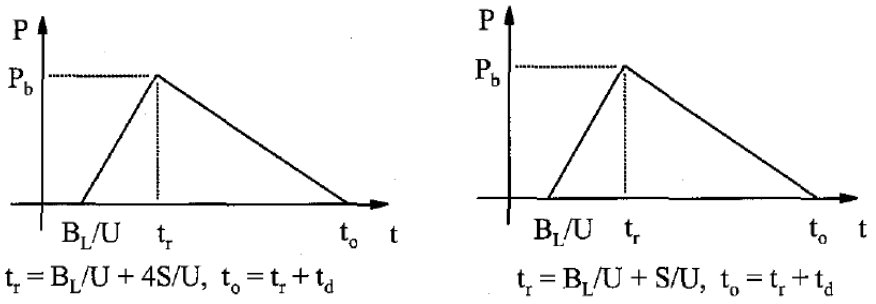

(a) Based on TNO Green book (b) Based on UFC3-340-02

Figure 2-13 Pressure-time graph for rear wall (ASCE, 2010)

Chapter 3. Comparative Analysis of Empirical Gas Explosion Models

In this chapter, comparisons of gas explosion methods will be analyzed. Offshore industry plants have more complex situations and higher risk so that the use of computational fluid dynamics (CFD) is required for better understanding of gas explosion and more accurate modeling. Unlike offshore plants, onshore plants having simpler plans adopt an empirical model for predicting the effects by explosions. Because this thesis focuses on onshore industry, the TNT equivalency method (TNT EM), the TNO multi-energy method (TNO MEM), and the Baker-Strehlow-Tang (BST) method are compared. The TNT equivalency method is chosen because the mass of TNT is still referred in the conventional blast resistant guideline. Comparisons with TNT EM and other methods show the different results caused by different explosions. Because the TNO MEM and the BST method are most widely used in onshore industry (Turner and Sari, 2012), they are selected for comparison. These methods are compared based on overpressure, impulse and positive durations, which are main effects by explosions.

3.1 Standard of comparison

Unlike the TNT EM, which has a single graph, the TNO MEM and BST method have various class and Mach numbers. These class number and Mach numbers must be determined separately because the blast parameters are dependent on the ‘number’. The overpressure, the most important factor in blast resist designs, is used for deciding the class number. Specifications used in famous petroleum factories for blast resistant designs are referred and the harshest condition is used (Lee and Lee, 2012); the distance from the center of

a gas explosion is 30.48 m (100 ft) and combustion energy is equivalent energy of TNT 1 tonf. The overpressure obtained by the TNT EM is used to determine the class/Mach number of the TNO ME or BST method. The scaled distance of the TNO ME or BST method requires the combustion energy of a gas cloud. With the addition of a corresponding gas cloud to the TNT mass, the combustion energy of the cloud could be obtained. For a stoichiometric hydrocarbon-air mixture, the combustion energy has such a similar value (3.5 MJ/m^3) so that the type of gas is irrelevant. The corresponding volume of gas cloud and the combustion energy are obtained by **Eqs. (2-4)** and **(2-5)**. Other blast parameters, duration and impulse, are compared in conjunction with the determined class/Mach number or scaled distance. The overpressure, duration, or impulse is compared via the class/Mach number or the scaled distance.

Because the Unified Facilities Criteria (UFC, 2008) gives two different explosive graphs based on the expansion type, i.e., spherical or hemispherical explosions; the two types of gas explosions are compared in the TNT equivalency method. The TNO multi-energy method was made in the case of the hemispherical explosion, so the TNO multi-energy method is used only in cases where hemispherical explosions are compared. The BST method, on the other hand, has different combustion energy depending on expansion type. Hemispherical explosions have two times the combustion energy of spherical explosions. This fact is considered when calculating the scaled distance.

In given conditions, TNT EM is used for determining the gas explosive overpressure. The scaled distance of TNO ME and BST methods are calculated. Under same overpressure, the class and Mach number are determined at the scaled distance by either the TNO ME or BST method. Other main factors included the duration and impulse, which are also computed with the class/Mach number and the scaled distance. More details in this regard are described in **Appendix A**.

In accordance with the calculations, the combustion energy of gas is 21.875×10^9 J, corresponding to 1 tonf of TNT. The scaled distance by TNT

EM or TNO MEM is 8 or 0.5. The BST method is divided in case of spherical or hemispherical explosions and the results are 0.5 or 0.4. These results are summarized in **Table 3-1**. In the table, 'Spherical' means special explosion and 'Hemispherical' is hemispherical explosion.

Table 3-1 Conditions used for comparison

R		30.48 m (100 ft)	
W_{TNT}		1000 kg	
E_{comb}		21.875×10^9 J	
Z	TNT EM	8	
$\bar{R}$	TNO MEM	0.5	
	BST method	Spherical	0.5
		Hemispherical	0.4

3.2 Overpressure (P_{SO})

3.2.1 Number

The overpressures are also calculated via the class and Mach number. Following the calculation, the overpressure by TNT equivalency method is 68.95 kPa and 89.63 kPa, in spherical explosion and hemispherical explosion, respectively (**Table 3-2**). Those are corresponding to the class number between 6 and 7, and the Mach number between 0.7 and 1.0. These numbers would be used for comparisons from now. The overpressure by TNO MEM and BST method is summarized in **Tables 3-2**, **3-3** and **3-4**, respectively.

Table 3-2 Overpressure by TNT equivalency method

Scaled distance		8
P_{SO} (kPa)	Spherical	68.9
	Hemispherical	89.6

Table 3-3 Overpressure by TNT equivalency method

Class number ($\bar{R}$=0.5)	1	2	3	4	5	**6**	**7**	8	9	10
P_{SO} (kPa)	1.0	2.0	5.1	10.1	20.3	**50.7**	**94.2**	192.5	202.7	202.7

Table 3-4 Overpressure by Baker-Strehlow-Tang method

M_w		0.2	0.35	**0.7**	**1**	1.4	2	3	4	5.2
P_{SO} (kPa)	Spherical ($\bar{R}$=0.5)	5.4	16.2	**50.7**	**83.1**	101.3	101.3	101.3	101.3	101.3
	Hemi-spherical ($\bar{R}$=0.4)	6.1	19.3	**58.8**	**101.3**	131.7	141.9	141.9	141.9	141.9

Note: M_w is Mach number

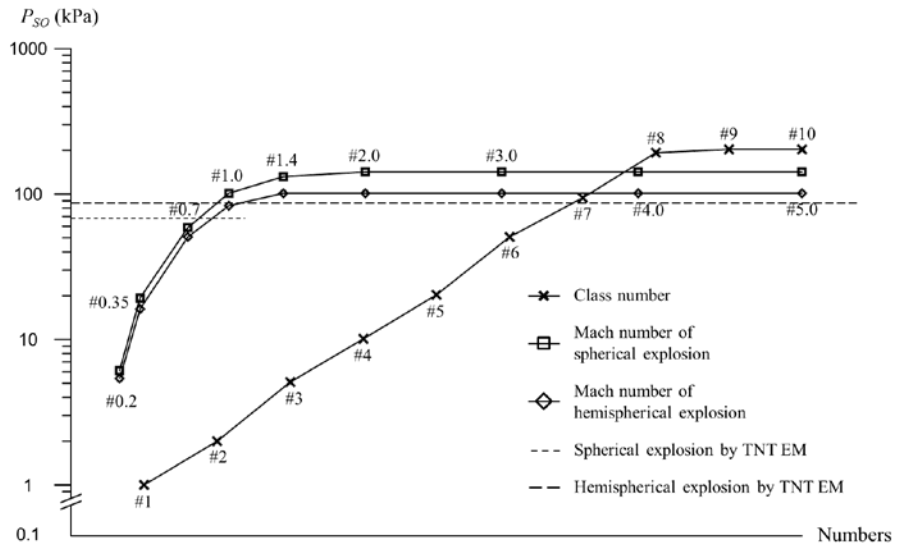

Figure 3-1 Peak overpressure via the class number or Mach number

In TNT equivalency and BST methods, the peak overpressure has different value according to a type of explosion expansion. It is guessed the shock wave reflected on the ground contributes to different peak overpressure. When an explosion occurs above the ground, the front shock wave, which is reflected on the ground, passes with later shock. This phenomenon is called 'Mach reflection', and the wave front is called the Mach stem, which usually has higher overpressure than one by a general explosion.

The peak overpressure of TNO ME and BST methods do not increase any more above certain number. It shows the gas explosion had similar effect till certain degree. While largest gas overpressure is obtained by TNO MEM (**Figure 3-1**), TNO MEM generally provided smaller overpressures than BST method. Explosions which have the class or Mach number larger than 7 or 1.0 in TNO MEM or BST method, respectively are called strong explosions. Strong explosions rarely occurred in on/offshore industry, so it is assumed BST method would make conservative design in general blast resistant design.

3.2.2 Distance

Next, overpressures are compared with an increase of various distances. The overpressure is checked at the distance from the center per 15.2 m (50 ft). Over 213 m (700 ft), distance increases per 30.5 m (100 ft), because the scaled indexes shows similar values. The class number 5 and Mach number 0.35 are also referenced as examples of weak gas explosions. The overpressures in case of spherical or hemi-spherical explosions are summarized in **Tables 3-5** and **3-6**, respectively. Actually, the real variable is the scaled distance. As a result, methods with the same combustion energy were compared with various distances. This assumption will be applied up until the end of this chapter.

Table 3-5 Overpressure by TNT EM and BST methods in case of spherical explosion

Distance	P_{SO} (kPa)			
m (ft)	TNT EM	BST method		
		#0.35	#0.7	#1.0
15.2 (5)	344.7	20.3	70.9	125.6
30.5 (100)	**68.9**	16.2	**50.7**	**83.1**
45.7 (150)	34.5	10.1	34.5	50.7
61.0 (200)	20.7	10.0	30.4	32.4
76.2 (250)	15.2	7.1	22.3	22.3
91.4 (300)	11.0	6.1	19.3	18.2
107 (350)	9.0	5.1	15.5	14.2
122 (400)	8.3	5.0	14.2	13.2
137 (450)	6.9	3.7	12.2	12.2
152 (500)	6.2	3.3	10.1	11.1
168 (550)	5.5	3.2	9.1	10.1
183 (600)	4.8	3.2	10.1	9.1
198 (650)	4.1	2.6	9.1	8.3
213 (700)	3.9	2.4	8.1	7.1
244 (800)	3.4	2.3	7.1	6.3
274 (900)	2.8	2.0	6.1	6.1
305 (1000)	2.5	1.8	5.4	5.1
366 (1200)	2.1	1.5	4.6	4.1
396 (1300)	1.6	1.3	4.1	3.6

Table 3-6 Overpressure by three methods in case of hemispherical explosion

Distance	P_{SO} (kPa)						
m (ft)	TNT EM	TNO MEM			BST method		
		#5	#6	#7	#0.35	#0.7	#1.0
15.2 (5)	482.6	-	-	-	21.8	68.9	125.6
30.5 (100)	**89.6**	20.3	**50.7**	**94.2**	19.3	**58.8**	**101.3**
45.7 (150)	42.7	14.2	40.5	63.8	13.2	42.6	69.9
61.0 (200)	27.6	12.2	32.9	49.6	10.6	35.5	43.6
76.2 (250)	20.7	8.3	22.3	27.4	10.0	30.4	32.4
91.4 (300)	13.8	7.3	18.2	22.3	7.4	24.3	24.3
107 (350)	12.4	6.3	15.2	16.2	6.1	20.3	19.3
122 (400)	10.3	6.1	15.2	14.2	5.4	17.2	16.2
137 (450)	8.3	5.1	12.2	12.2	5.1	15.5	14.2
152 (500)	8.2	4.4	10.3	10.3	5.0	14.2	13.2
168 (550)	6.9	4.2	10.1	10.1	4.1	12.2	12.2
183 (600)	6.3	4.1	9.4	9.4	3.7	12.2	12.2
198 (650)	6.2	3.3	8.1	8.1	3.4	10.1	11.1
213 (700)	5.5	3.1	7.1	7.1	3.2	9.1	10.1
244 (800)	4.8	3.0	6.6	6.6	2.9	9.1	8.1
274 (900)	3.7	2.5	6.1	6.1	2.4	8.1	7.1
305 (1000)	3.4	2.3	5.1	5.1	2.3	7.0	6.3
366 (1200)	2.8	2.0	4.1	4.1	1.9	5.4	5.1
396 (1300)	2.3	2.0	3.5	3.5	1.7	5.1	4.9

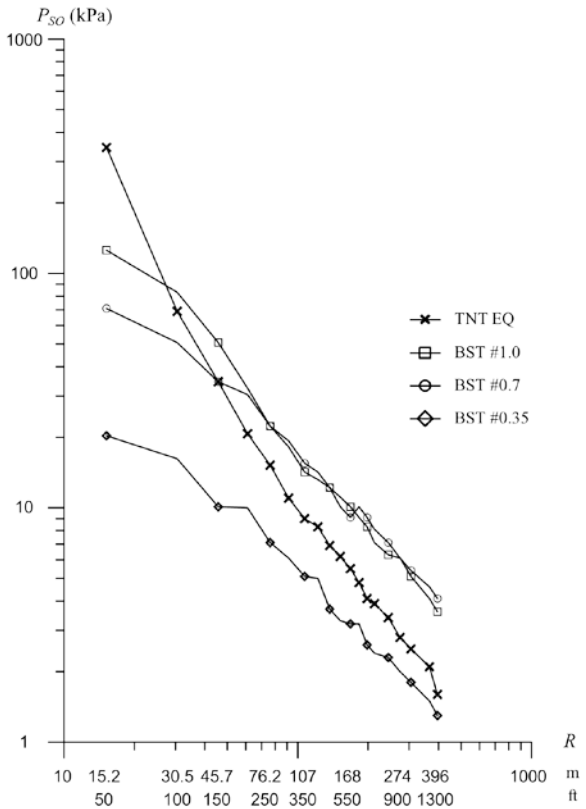

(a) Spherical explosion

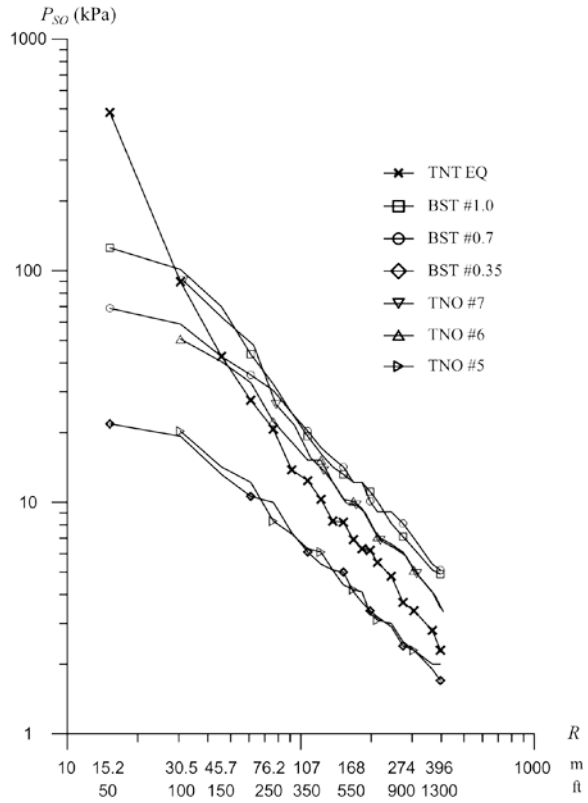

(a) Hemispherical explosion

Figure 3-2 Peak overpressure predicted by gas explosive methods

The slope of the TNT EM is steeper while the TNO MEM and BST method showed similar slopes. The overpressure shows drastic decreases until about 30.48 m (100 ft). From 45.7 to 61 m (from 150 to 200 ft), the overpressures of the TNT EM becomes even less than those of class number 6, 7, Mach number 0.7 or 1.0 (**Figure 3-2**). It is suggested that design engineers determine the distance from the explosion center carefully. If a building is far away from the explosion center, a blast resistant design based on the TNT EM could be dangerous.

As distances increases, strong explosions of the TNO MEM or BST method converge. With far distances, the TNO MEM and BST method also shows overlap, especially in regards to weak explosions. In close distances, the overpressure of high class/Mach number is approximately double. The class/Mach number 6 and 0.7 or the class/Mach number 7 and 1.0 had similar overpressures. The BST method provides slightly more conservative results. Similarly to the TNT EM methods described previously, it is assumed that the distance from the center is more important than the type of methods in the case of the TNO MEM, and BST method. Since there is a clear gap between weak and strong explosions, judgments on particular types of explosions must be important.

3.3 Positive duration (t_d)

3.3.1 Number

In this section, the duration of the positive phase is compared with regards to each method. The TNT EM and TNO MEM suggest graphs of the scaled duration while the scaled impulse, rather than the scaled duration is suggested by the BST method. In **Eq. (2-8)**, while calculating the impulse of TNO MEM, it is assumed that the BST method also adopts the same procedures. As explained above, the TNO MEM is compared only in the case of hemispherical explosions. In the original condition, the duration of the three various methods is summarized in **Table 3-7**.

Table 3-7 Duration by three methods in case of hemispherical explosion

Explosion type	t_d (sec)						
	TNT EM	TNO MEM			BST method		
		5	6	7	0.35	0.7	1.0
Spherical	0.029	-	-	-	0.109	0.042	0.026
Hemispherical	0.029	0.124	0.068	0.052	0.139	0.053	0.031

Note: Type is the expansion type of explosion

Based on **Table 3-7**, the higher class/Mach number has a shorter duration. It also seems that stronger gas explosions have shorter explosions. Moreover, the hemispherical explosions have longer durations than the spherical explosions of the BST method. This result seems contradictory to previous analysis. However, this inconsistency could be accounted for in terms of combustion energy. Since the combustion energy of hemispherical explosions are two times that of spherical ones; it is to be expected that the duration of the explosions increased.

3.3.2 Distance

Duration with increases in distance is also compared. The same procedure used in TNT EM is applied. The durations in the case of the spherical and hemi-spherical explosion are summarized in **Tables 3-8** and **3-9**, respectively.

Table 3-8 Duration by TNT EQ and BST methods in case of spherical explosion

Distance	t_d (sec)			
m (ft)	TNT EM	BST method		
		#0.35	#0.7	#1.0
15.2 (5)	0.016	0.157	0.050	0.032
30.5 (100)	**0.029**	0.109	**0.042**	**0.026**
45.7 (150)	0.031	0.112	0.037	0.028
61.0 (200)	0.035	0.099	0.035	0.035
76.2 (250)	0.039	0.090	0.035	0.037
91.4 (300)	0.042	0.087	0.033	0.037
107 (350)	0.042	0.091	0.034	0.039
122 (400)	0.043	0.086	0.035	0.040
137 (450)	0.046	0.097	0.035	0.036
152 (500)	0.047	0.106	0.036	0.037
168 (550)	0.048	0.098	0.040	0.040
183 (600)	0.049	0.096	0.035	0.045
198 (650)	0.051	0.098	0.035	0.038
213 (700)	0.052	0.102	0.035	0.041
244 (800)	0.055	0.103	0.039	0.045
274 (900)	0.056	0.105	0.041	0.042
305 (1000)	0.057	0.097	0.040	0.043
366 (1200)	0.059	0.100	0.039	0.046
396 (1300)	0.061	0.108	0.038	0.045

Table 3-9 Duration of hemispherical explosion predicted by three methods

Distance	t_d (sec)						
m (ft)	TNT EM	TNO MEM			BST method		
		#5	#6	#7	#0.35	#0.7	#1.0
15.2 (5)	0.020	-	-	-	0.236	0.104	0.053
30.5 (100)	**0.029**	0.124	**0.068**	**0.052**	0.139	**0.053**	**0.031**
45.7 (150)	0.036	0.115	0.066	0.047	0.142	0.052	0.032
61.0 (200)	0.042	0.121	0.068	0.052	0.133	0.049	0.041
76.2 (250)	0.043	0.121	0.069	0.055	0.107	0.044	0.044
91.4 (300)	0.044	0.121	0.070	0.058	0.121	0.042	0.044
107 (350)	0.048	0.121	0.070	0.059	0.118	0.042	0.046
122 (400)	0.049	0.121	0.070	0.059	0.116	0.041	0.050
137 (450)	0.052	0.121	0.070	0.065	0.115	0.043	0.049
152 (500)	0.055	0.121	0.070	0.066	0.108	0.044	0.051
168 (550)	0.056	0.121	0.070	0.068	0.115	0.045	0.048
183 (600)	0.057	0.121	0.072	0.070	0.119	0.043	0.044
198 (650)	0.059	0.121	0.073	0.070	0.121	0.045	0.042
213 (700)	0.060	0.121	0.073	0.070	0.124	0.050	0.050
244 (800)	0.062	0.121	0.073	0.072	0.122	0.044	0.055
274 (900)	0.065	0.121	0.073	0.073	0.129	0.044	0.052
305 (1000)	0.066	0.121	0.074	0.073	0.130	0.050	0.057
366 (1200)	0.068	0.121	0.074	0.074	0.123	0.051	0.056
396 (1300)	0.070	0.121	0.075	0.075	0.124	0.053	0.056

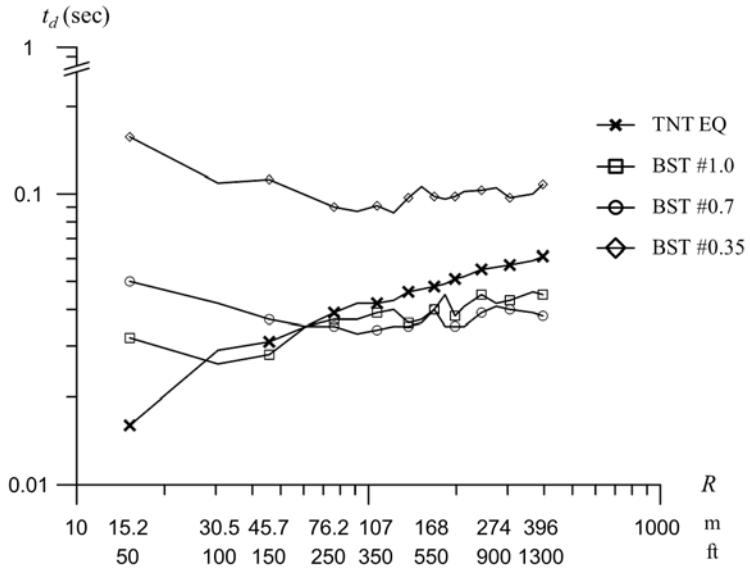

(a) Spherical explosion

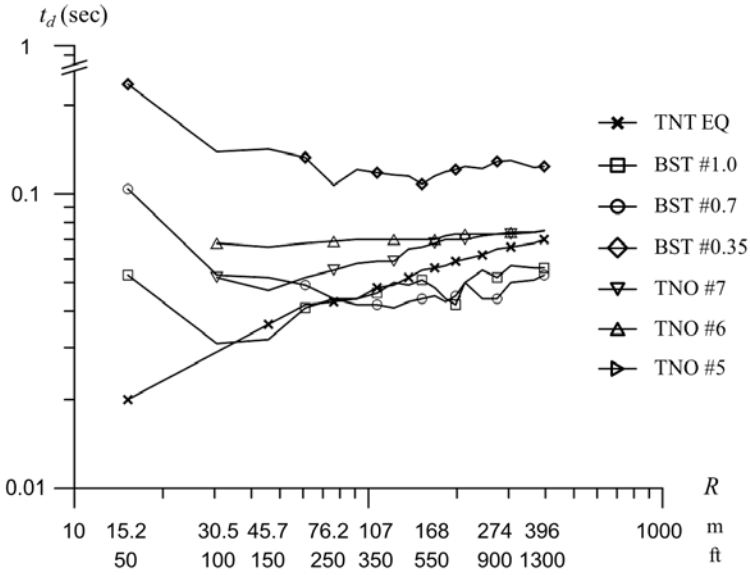

(b) Hemispherical explosion

Figure 3-3 Positive duration predicted by gas explosive methods

The duration of the TNT EM is shorter than that of the TNO ME and BST methods except in the case of Mach number 1.0. The duration of the TNO ME or BST method is up to four times longer. The short duration of the TNT EM is expected due to the high reactivity of TNT. The TNT usually detonates with a high reaction time due to its having a short intramolecular. When the velocity of combustion is faster than speed of sound, this phenomenon is called ‘detonation’. It is considered a detonation in the TNO ME or BST method when there is a class number 7, or Mach number 1.0. Smaller numbers are usually mentioned as deflagration. It is worth noticing the duration of TNT is similar to the detonation of a gas explosion; the class number 7 or Mach number 1.0.

The duration by the TNO MEM and BST method have different shapes while the duration by the TNT EM increases non-linearly in accordance with the increasing distance. The duration of the two methods converged after experimenting with both decreases and increases, similar to **Figure 2-3 (a)**. The shapes of the BST method seem less smooth than that of the TNO MEM (**Figure 3-3**). The assumed duration of the BST method is converted by this simplified impulse ($I=P_{SO}\times t_d/2$). Real gas explosive impulses, overpressures and durations might have more complex interrelations. Since the duration is dependent on the class/Mach number as outlined above, it is important for people to take this into consideration when attempting to predict the strength of gas explosions.

3.4 Impulse (I_W)

3.4.1 Number

In this section, the impulse of positive phase for each method will be compared. The TNT EM and BST method provides a scaled index, **Figures 2-2** and **2-5**, but the TNO MEM only suggests a calculation equation, subscribe in **Eq. (2-8)**. As explained above, the TNO MEM is employed only in comparison involving only hemi-spherical explosions. Under the original conditions, the durations of the three methods were summarized in **Table 3-10**.

Table 3-10 Impulse by three methods in case of hemispherical explosion (Pa·sec)

Type	TNT EM	TNO MEM			BST method		
		5	6	7	0.35	0.7	1.0
Spherical	628	-	-	-	886	1063	1063
Hemispherical	897	1258	1728	2472	1340	1563	1563

As expected, hemispherical explosions, which larger overpressures and longer durations, have more impulse than spherical explosions. The BST method is conservative in terms of overpressure; however, the impulse of the BST method is smaller than that of the TNO MEM. As explained above, a simplified triangular graph of overpressure and impulse is not precise enough for a gas explosion. This simplification is expected to result in conservative results. The TNT EM, then, ensures smaller impulses than the other methods even with similar overpressures and durations.

3.4.2 Distance

The varying impulses with increased in distance are also compared. The same procedure used in the TNT EM is applied. The durations in the case of spherical and hemi-spherical explosion are both summarized in **Table 3-11** and **Table 3-12**, respectively.

Table 3-11 Impulse by TNT EM and BST method in case of spherical explosion

Distance	I_W (Pa·sec)			
m (ft)	TNT EM	BST method		
		0.35	0.7	1.0
15.2 (5)	1077	1595	1772	2003
30.5 (100)	**628**	886	**1063**	**1063**
45.7 (150)	449	567	638	709
61.0 (200)	305	496	532	567
76.2 (250)	269	319	390	408
91.4 (300)	206	266	319	337
107 (350)	197	230	266	275
122 (400)	179	213	248	266
137 (450)	135	183	213	216
152 (500)	126	177	184	206
168 (550)	117	160	181	200
183 (600)	112	156	177	204
198 (650)	108	129	160	160
213 (700)	90	124	142	147
244 (800)	81	121	140	142
274 (900)	72	106	124	128
305 (1000)	63	89	106	109
366 (1200)	54	76	89	94
396 (1300)	45	71	78	82

Table 3-12 Impulse by three methods in case of hemispherical explosion

Distance	I_W (Pa·sec)						
m (ft)	TNT EM	TNO MEM			BST method		
		5	6	7	0.35	0.7	1.0
15.2 (5)	1525	-	-	-	2568	3572	3349
30.5 (100)	**897**	1258	**1728**	**2472**	1340	**1563**	**1563**
45.7 (150)	628	819	1347	1507	938	1116	1116
61.0 (200)	467	734	1123	1303	710	871	893
76.2 (250)	377	501	770	754	536	670	714
91.4 (300)	314	440	638	643	447	514	536
107 (350)	278	379	532	482	357	424	447
122 (400)	269	367	532	422	313	357	402
137 (450)	206	306	425	393	290	335	346
152 (500)	197	263	362	343	268	313	335
168 (550)	179	251	354	346	232	272	290
183 (600)	162	245	338	330	223	259	268
198 (650)	153	202	298	284	208	228	232
213 (700)	135	190	261	248	201	228	252
244 (800)	117	183	242	236	179	201	223
274 (900)	108	153	223	223	156	179	185
305 (1000)	101	141	188	186	152	176	179
366 (1200)	90	122	151	151	118	137	141
396 (1300)	81	122	133	133	107	134	137

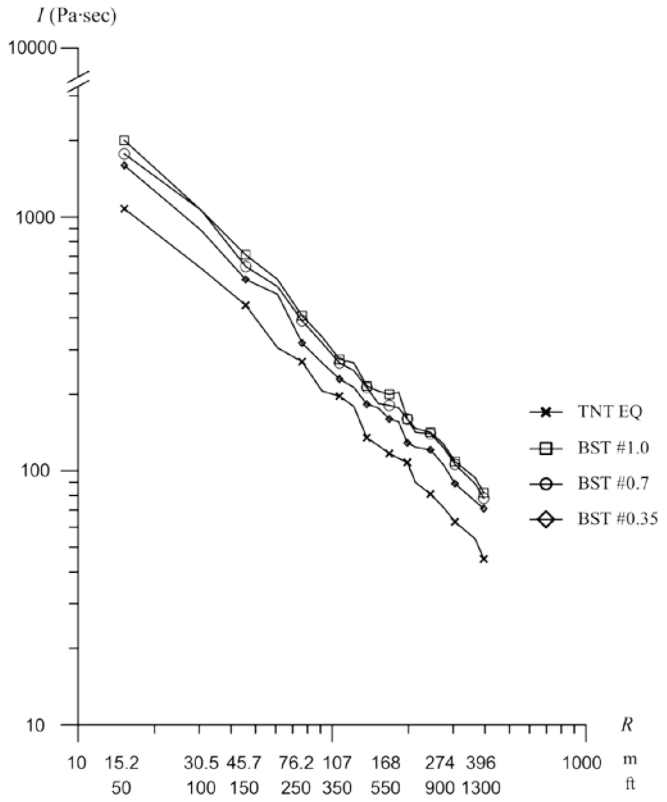

(a) Spherical explosion

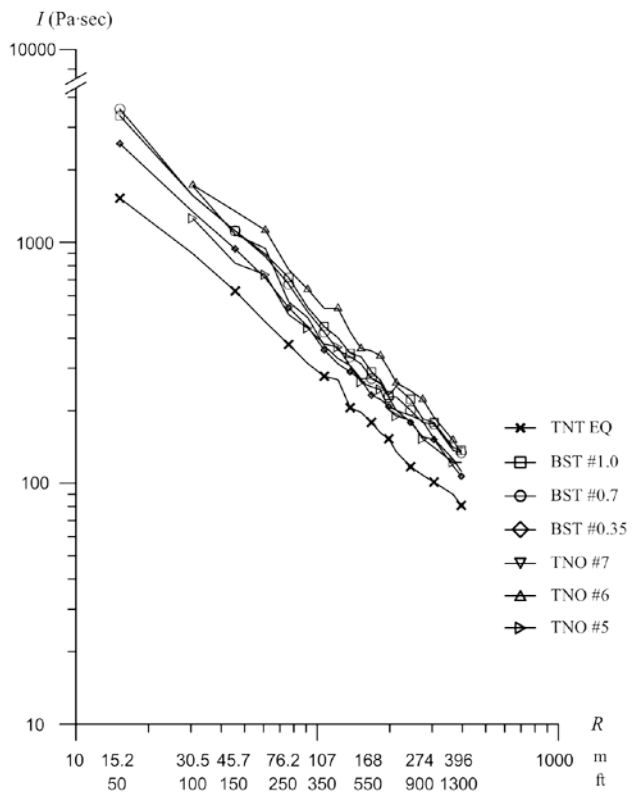

(a) Hemispherical explosion

Figure 3-4 Positive impulse predicted by gas explosive method

In all of these cases the impulse decrease relatively linearly (**Figure 3-4**). As showed above, the TNT EM provides the smallest impulse. American Society of Civil Engineering (ASCE) suggests one analysis method, which estimates the damage level of a structure using pressure-impulse diagrams. Based on **Tables 3-11** and **3-12**, the damage of structures could be underestimated when the TNT EM is employed. It is assumed that this is a result of the short duration of the TNT EM. Weak or strong explosions have the tendency of convergence in the TNO ME and BST methods. The gap between weak and strong explosions is narrow in comparison to that of the overpressure. In the case of closer distances, however, the range of impulse following the class/Mach number is still considerably varied, thus, the initial strength of a gas explosion should be determined carefully.

3.5 Shape of blast wave

When gas explosions occur, the emitted energy expands as waves, blast waves. As shown above, the blast wave is described with the peak overpressure and duration. For convenience, blast waves are simplified as triangular shapes. TNO multi-energy method especially suggests three types of blast waves based on the scaled distance and the class number (right top of **Figure 2-3 (a)**). Because of the peak overpressure and duration, the changes of blast effects could be realized easily. TNT equivalency and TNO ME methods are compared with the shape of blast wave. When results of gas explosions are predicted by TNO MEM, the shapes of blast waves are also done by the method. TNT equivalency method does not suggest any shapes, so simplified triangular shapes are used considering that the TNT usually detonates.

The TNO multi-energy method suggests the scaled values from the scaled distance of 0.23, but the scaled distance at 15.2 m (50 ft) was less than 0.23. Instead, overpressures and durations was calculated at the scaled distance of 0.23. The overpressure or durations of explosions were written behind they or x axis.

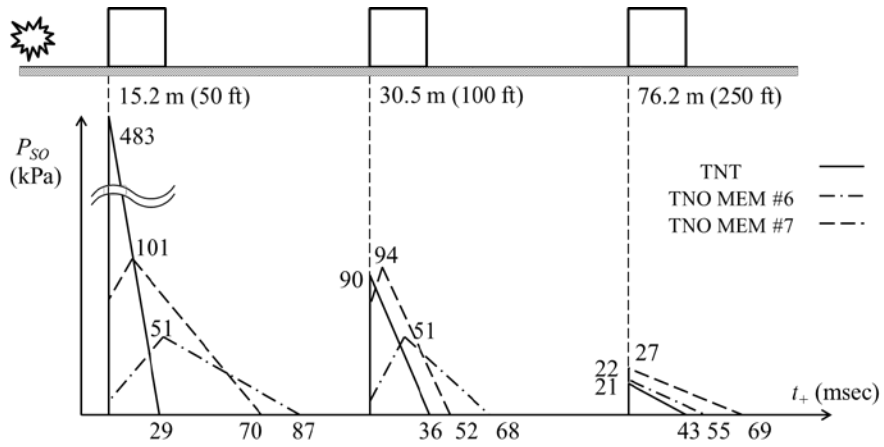

Figure 3-5 Shape of blast waves (TNT EM vs. TNO MEM)

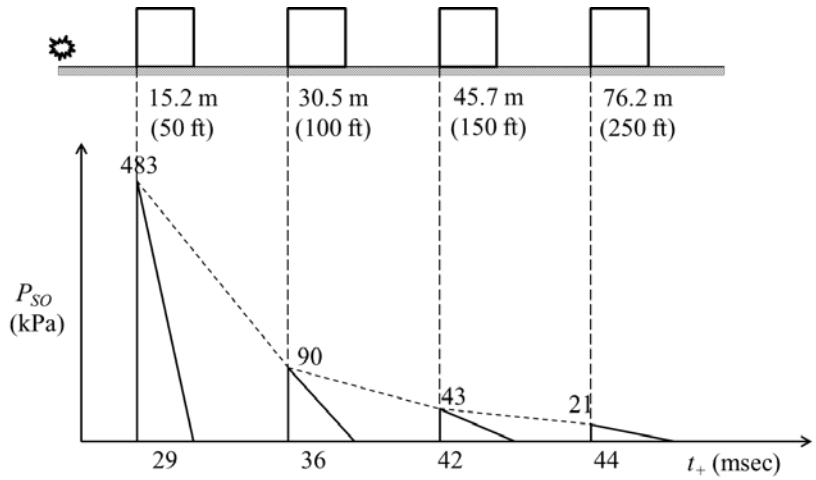

Figure 3-6 Shape of blast waves by TNT EM (via the distance)

Figures 3-5 and **3-6** summarize analysis explained above. Additionally, as the distance became far enough, TNO MEM predicted blast waves reached the peak overpressure without rising time.

Chapter 4. Comparative Analysis of Blast Resistant Design Using Various Empirical Models

4.1 Scope of blast resistant design

In this chapter, three empirical methods are applied to a blast resistant design and compared. In onshore industry, facilities are usually highly concentrated and the high density of equipment results in additional collapses. For example, the explosion of a polyethylene unit made a control building collapsed in Pasadena, in 1989. In Texas, 2005, an isomerization unit exploded and this destroyed trailers used as temporary offices. To protect lives and minimize damages, buildings in plants are designed to withstand explosions. Even if the buildings are not occupied, some companies consider implementing blast resistant design in main buildings to minimize the effects of explosions on operating plants. Therefore, blast resistant design is carried out for almost all buildings in onshore plants.

Plants recently constructed in South-East Asia apply the PC structure to reduce cost and shorten the construction period. Connections are main considerations because they determine the performance of structures. Connections of line members like beams and columns have been studied much. Because blast resistant connections of PC walls still need further study, PC wall connections with angles are designed for blast resistance. General blast resistant design is based on strength design. For convenience, the capacity of blast resistant connections is used to determine the number of connections per each method. The number of connections is used to compare methods. Simple unit models in the finite element analysis (FEA) program are analyzed in accordance with blast loads by three gas explosive overpressure

methods: TNT EM, TNO MEM and BST method. Results from the FEA program are used to study the behavior of unit models and check PC panel connection design.

4.2 Determination of blast load

4.2.1 Overpressure

Gas explosions have different results depending on a variety of different conditions, including: the distance from the center, the size of the vapor cloud, the reactivity of the gas, the density of the equipment and so on. A virtual scenario is made to determine the overpressure of each method. This scenario is created with reference to two vital texts (CCPS, 2004; Casal, 2010).

Propane gas was split as a result of human error. About 25,000 kg of propane gas was assumed to have been spilt, which resulted in the formation of 9,000 m^2 of propane vapor cloud. The overpressure was evaluated every 80 m apart. The flame would expand as a 3D shape, and the equipment was installed in vapor densely. The explosion in a hemi-spherical shape was observed.

4.2.1.1 TNT equivalency method (TNT EM)

Before calculating the TNT equivalent mass, the flash fraction of the fuel must first be obtained through **Eq. (4-1)**. Fuel mass is calculated by multiplying the flash fraction with the mass of the propane gas, $W_{propane}$. Because the vapor cloud includes the mist and the aerogel of fuel in the cloud, it is doubled ($W_{fuel} = 2 \times F \times W_{propane}$). The TNT equivalency of the fuel mass is calculated with the yield ratio, fuel mass, as well as the combustion heat ratio of both the fuel and the TNT. Hence the TNT equivalent mass is obtained by **Eq. (4-1)**.

$$F = 1 - \exp\left(\frac{C_p \triangle T}{L}\right) \qquad (4\text{-}1)$$

Where,

F	:	flash fraction
C_p	:	mean specific heat for liquid propane, 2.41 kJ/kg/K
ΔT	:	gas of temperature
L	:	latent heat for propane = 410 kJ/kg

$$W_{TNT} = \alpha_0 \frac{W_{fuel} H_{fuel}}{H_{TNT}} \quad (4\text{-}2)$$

Where,

W_{TNT}	:	equivalent mass of TNT, kg
α_0	:	yield ratio, 0.03
W_{fuel}	:	fuel mass in vapor, kg
H_{TNT}	:	combustion heat of TNT J/kg
H_{fuel}	:	combustion heat of fuel, J/kg

The scaled distance by TNT equivalent mass, *Z*, was obtained by **Eq. (2-1)**. In accordance with **Figure 2-2(b)**, the peak overpressure is 43.4 kPa, while the duration is 0.065 sec. More detailed calculations are subscribed in **Appendix B**.

4.2.1.2 TNO multi-energy method (TNO MEM)

According to the TNO gas classification, propane gas is classified as having medium reactivity. The class number is determined based on **Table 2-2**. The type of flame expansion is 3D, and the obstacle density is 3D because of the dense equipment involved. The class number is 3 or 4. In this particular scenario the class number is determined to be 4 to result in a conservative design. Almost all stoichiometric fuel-air mixtures have about 3.5 MJ/m^3 of combustion heat. By multiplying 3.5 MJ/m^3 and volume of the VC, the combustion energy is 3.15×104 MJ. As the distance is 80 m, the scaled distance is calculated as 1.2 following Sach's scaling law, **Eq. (2-2)**. The overpressure and duration are calculated in conjunction with **Figure 2-3**, **Eqs.**

(2-6) and **(2-7)**. The overpressure is 5.47 kPa, and duration is 0.24 seconds. More details are subscribed in **Appendix B**.

4.2.1.3 Baker-Strehlow-Tang (BST) method

Following the BST method, the scaled distance, Mach number, and overpressure are to be determined following the same procedures as the TNO MEM. It is assumed that the energy of the combustion is doubled if the explosion is hemi-spherical (Melani et al, 2004). The combustion energy is 6.3×104 MJ and the scaled distance is 0.94. The Mach number is 0.5, based on the Pierorazio et al. matrix, **Table 2-4**. A Mach number of 0.5 is not considered in the original BST curves suggested by Tang and Baker (1999). Consequently, the overpressure in this case is calculated by using the interpolation between a Mach number of 0.35 and that of 0.7 (**Figure 2-5**). The BST method does not give any curves estimating the duration of explosion. Instead, a simplified overpressure triangular force-duration graph is used. The positive impulse is determined based on **Figure 2-5** and **Eq. (2-9)**. The overpressure is 19 kPa at 0.94 of scaled distance and the duration is 0.42 seconds. More details are described in **Appendix B**.

4.2.2 Static blast load

A blast load caused by a gas explosion is calculated using equations in the ASCE (2010). The incidence angle of a blast wave determines its blast load, but in blast resistant designs, the angle remains at zero for a conservative design. A blast load is maximized when a blast wave is facing a wall. Here the two most conservative examples are considered in virtue of the fact that it is hard to accurately predict where gas explosions will occur. These include applied blast loads from both perpendicular and longitudinal directions of a structure (**Figure 4-1**).

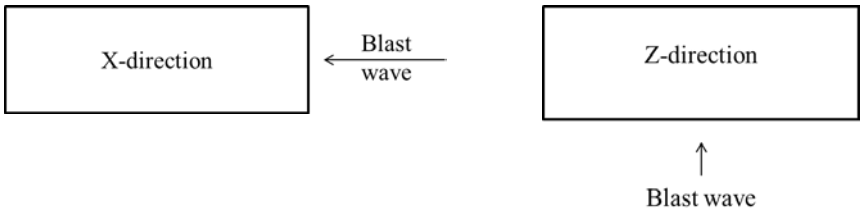

(a) Load case A (b) Load case B

Figure 4-1 Directions of blast wave caused by gas explosion

In the petrochemical industry, the static design approach (in which blast dynamic loads are considered as static loads) is a common approach because of its being easy to use. This approach could result in conservative designs (ASCE, 2010). Design engineers use the maximum resistance, R_m, for calculating the static blast load and required dynamic pressure. The maximum resistance could be calculated by **Eq. (4-3)**. In the industrial field, designers determine a number of variables found on the right side of **Eq. (4-3)** within the information given. The maximum resistance, which is considered the required dynamic pressure or the static blast load, can be obtained in this way. More details are described in **Appendix C**.

$$\frac{F_O}{R_m} = \frac{\sqrt{2\mu_d + 1}}{\pi(\tau)} + \frac{(2\mu_d - 1)(\tau)}{2\mu_d(\tau + 0.7)} \qquad (4\text{-}3)$$

Where,

F_O : peak force, kN
R_m : maximum resistance of member
μ_d : y_m/y_e, ductility demand
y_m : maximum deflection
y_e : yield deflection
τ : t_d/t_n, ratio of load duration to natural period
t_d : duration of blast loading
t_n : natural period of structure

The reflected overpressure is used as the peak force, F_O. The reflection coefficient is obtained by **Eq. (2-12)**. The ductility demand, μ_d, varies depending on the various element types and the degree of response. Notably, precast wall panels are not included in the ASCE guidelines, but they may be considered as reinforced concrete (RC) components. The demanded ductility of RC a shear wall or diaphragm is 3.0. The duration of a blast load, t_d, is obtained by **Eqs. (2-19)** or **(2-21)** depending on the members involved. These two values remain dependent on the overpressure methods, that is, the TNT equivalency, the TNO ME and the BST method. In plant designs, the natural period of each member, t_n, is usually calculated with the equivalent variables of each member, i.e., the front wall, the sidewall or the roof (Biggs, 1964). In this thesis, equivalent mass of the beam, stiffness of simply supported beam and gross moment of inertia are used. The natural period of the unit wall is determined to be 0.071 sec.

Under the conditions outlined above, the blast load and the static load are calculated. The most important information, the peak overpressure and the duration, are obtained through three competing empirical methods. Even with the same overpressure, the static load is varied depending on the pertinent load cases and the location of members. The static load decreases and loads in Load case B increases more than in Load case A. The blast load calculated by the TNT EM, which suggests the highest overpressure, is the maximum. If the ductility ratio, μ_d, is set at 1.6 for RC components with shear force, applied load increases and becomes larger than blast load. This shows the ductility of members could increase or decrease the capacity of members. The applied blast loads in the front wall are changed in accordance with the direction of applied load. It may be caused by different clearing distance, which makes the equivalent duration of blast load, t_e, and the ratio of natural period and duration, τ, different. The overpressure, the blast load, and the static load in each case are summarized in **Table 4-1**.

Table 4-1 Blast load and required dynamic pressure by gas explosive methods

Method	Member	P_{SO} (kN/m^2)	Blast load (kN/m^2)	Required dynamic pressure (kN/m^2)	
				Load case A	Load case B
TNT EM	Front	43.4	100.6	59.2	71.1
	Side		40.9	33.3	33.3
	Roof		36.6	29.8	
TNO MEM	Front	5.4	11	11.0	11.2
	Side		5.3	5.9	5.9
	Roof				
BST method	Front	18.8	40.1	44.1	46.4
	Side		18.3	21.1	21.1
	Roof			21.2	

The ratio of overpressure is about 8:1:3.5 for TNT EM, TNO MEM and BST method. As the overpressure is converted to the required dynamic pressure, i.e., the equivalent static blast load, the ratio decreases to about 5:1:4 or 6:1:4 in Load case A or B.

4.3 Analysis of structural behavior under static blast load

4.3.1 Modeling

Concrete is assigned as material of members. In MIDAS Gen., concrete is used in reinforced, precast or prestressed concrete structures. Strength of concrete and sizes of members in modeling are set referred with general values in industry field. Material type of all members is concrete of 27 MPa. Element members are divided in columns, beams and walls, which are set as 300 × 300 mm, 300 × 500 mm, and 200 mm of thickness, respectively.

In modeling, element types of columns and beams are general line members. Generally, walls are assigned as wall members for considering shear force. In this thesis, plane members are used to consider out-of-plane deflection. MIDAS Gen. suggests ideal divided size of plane as 2~3 times of wall thickness. Plate members are meshed as 500 × 500 mm. Because node's

sharing makes analysis smooth and accurate, line members are meshed per 500 mm (**Figure 4-2**).

Modeling boundaries are fixed ends as PC members are generally constructed with fixed ends. Conditions of PC connections are depending on construction methods, workability, environment, or worker's experience. Because these make connections loose, connections between walls and columns, or between walls and ground beams are also modeled as hinged ends (**Figure 4-3**).

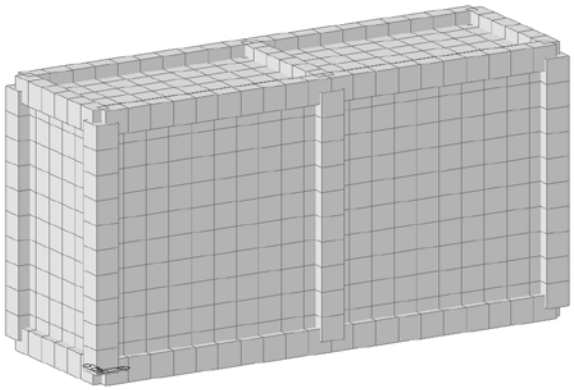

Figure 4-2 Modeling in MIDAS Gen

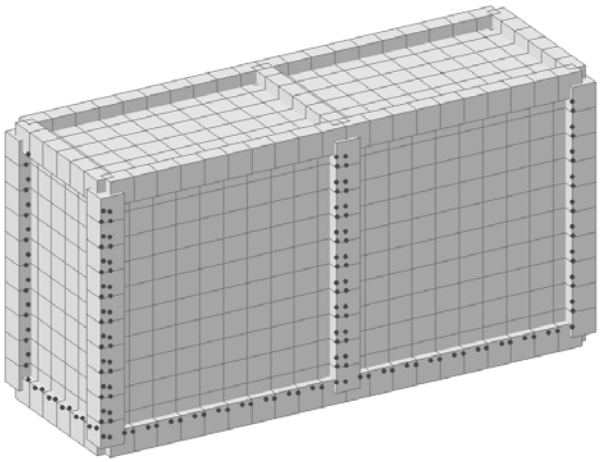

Figure 4-3 Hinged ends of structure (dots)

Dead and live load of the unit model is the same as in a plant design. Natural period of a structure is dependent on mass of the whole structure, so

equipment installed in a plant is assigned as dead load.

Explosions are assumed not to occur with other case, strong wind or earthquakes. Blast loads are combined with existing loads, only dead and live load. BSI (1997) and ASCE (2010) suggested load combination of dead load, live load and blast load with unity. Because results caused by different blast loads are expected to be rarely affected by dead load and live load, only blast load is applied when this model is analyzed.

4.3.2 Member name

Structural analysis is mainly purposed to research frame behavior caused by blast loads. The direction of applied blast load is mainly considered to explain structural behavior of frame rather than direction of gravity. Front wall, side wall, rear wall, and roof are named based on the direction of blast wave. When facing the front wall from the way blast waves progress, the wall on right or left side is named the right or left wall (**Figure 4-4**). Members of a unit model are described based on directions of blast load.

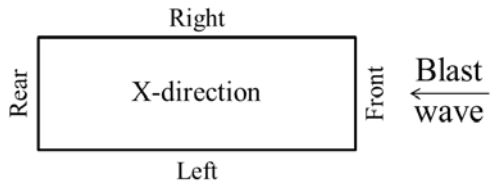

(a) Load case A

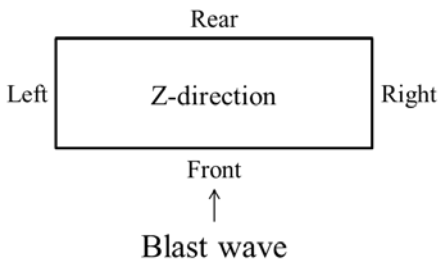

(b) Load case B

Figure 4-4 Direction of blast load

Behavior of this structure is analyzed based on blast directions and boundary conditions. The blast direction, Load case A or B is considered for explanation firstly. The different results caused by the boundary conditions, fixed or hinged ends, are also described.

4.3.3 Axial forces

First, axial forces on columns are dealt with. Axial forces on opposite columns are equally based on the centerline of the front wall. Columns on the front wall experience uplift axial force except the middle column on the front wall, in Load case B. Downward axial forces are applied to other columns (**Figure 4-5**). These uplift forces may be caused by blast load on the front and side wall. Pressure load may pull the front columns up and make the front wall deflected inside. Maximum axial forces are applied on rear columns and increased in Load case B. Middle columns of the front and rear wall seemed to react separately in Case B. The middle front or rear column in Case B endures significantly less axial forces than columns on side walls. When the boundary condition is changed from fixed to hinged ends, most axial forces applied on columns increased. The maximum axial forces of both cases are summarized in **Table 4-2**. The ratio of axial force is 4:1:3 or 5:1:4 in Load case A and 6:1:4 in Load case B. It is also similar to the ratio of required dynamic pressure.

Table 4-2 Maximum axial force on columns

Method	Load case	Axial force (kN)	
		Fixed	Hinged
TNT EM	Case A	-54.5	-54.6
	Case B	-473.6	-517.7
TNO MEM	Case A	-13	-10.6
	Case B	-75	-82
BST method	Case A	-40.8	-41
	Case B	-308.7	-337.4

Note: Negative sign (-) means downward axial force.

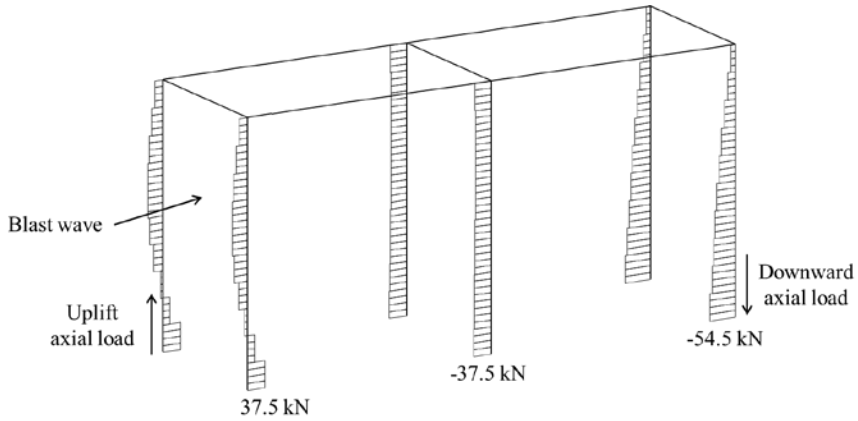

(a) Load case A (fixed end)

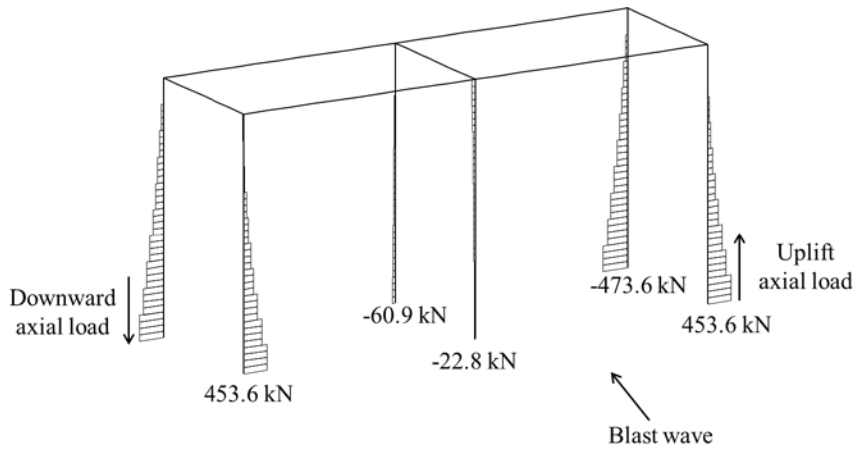

(b) Load case B (fixed end)

Figure 4-5 Axial forces of columns

4.3.4 Shear force

Shear forces concentrate on the middle members. Maximum shear force is applied to the middle columns in the largest wall and the middle beam on the roof, connecting two middle columns (**Figure 4-6**). Shear forces are changed depending on the load case and the boundary condition.

Shear forces acting on columns are analyzed first. Vertical shear force to walls is larger than horizontal shear force. It may be caused by blast load applied as pressure load vertically acting on walls. Some columns, included in the front (or rear) wall and the side wall, experience larger shear force when it is applied in the same direction as progressing blast waves. It is assumed that the blast load of the front wall governs on shear forces of the front (or rear) wall because the front wall endures larger blast load per area than the side walls. Maximum shear force is vertically applied to the middle columns of side walls in Load case A and the middle column of the front wall in Load case B. The maximum shear forces increase when the load case is B and the boundary condition is changed from fixed to hinged ends. Especially, the change of boundary condition causes increase of member shear force by about 80%.

The shear force is applied to the beams within only one direction, i.e., the direction of gravity. Blast load applied to the roof may make shear force acting on this direction. Maximum shear force is applied to the middle beam of the roof like a column. The shear force diagram (SFD) is drawn with point symmetry based on the centerline of the front wall. The absolute values remain the same, but the signs are the opposite. If the ends of the buildings are closed, shear force increases. When the boundary conditions are changed from fixed to hinged ends, the maximum shear force decreases, unlike the shear force on the columns. Instead, shear force applied on the other beams increases. Maximum shear forces applied to the columns and beams are summarized in **Table 4-3**. If the force is loaded from the exterior to the interior of the wall, this load is assumed to have a negative sign. The sign of

shear force also follows this way. When shear force acts in the same direction of force, the sign is negative. Because of the symmetric SFD, maximum beam shear force in Load case B acts in both negative and positive directions. In this case, the sign (-) means two opposite signs.

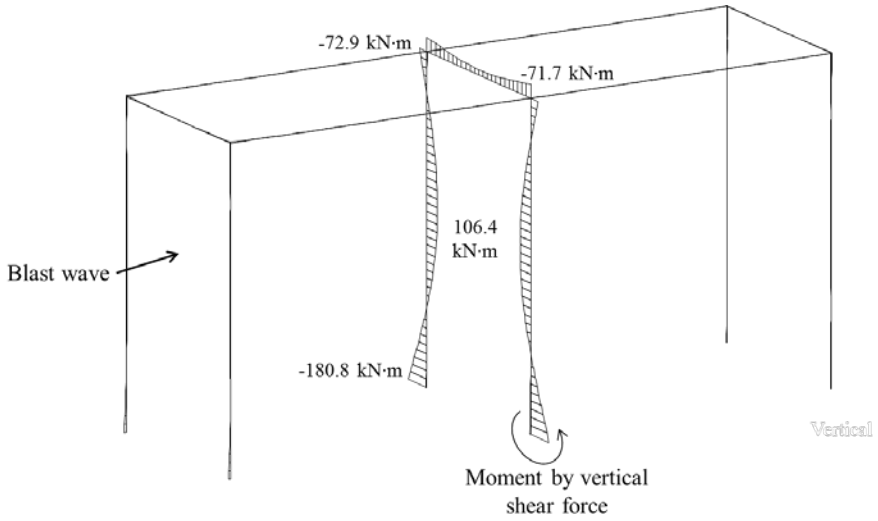

(a) Load case A

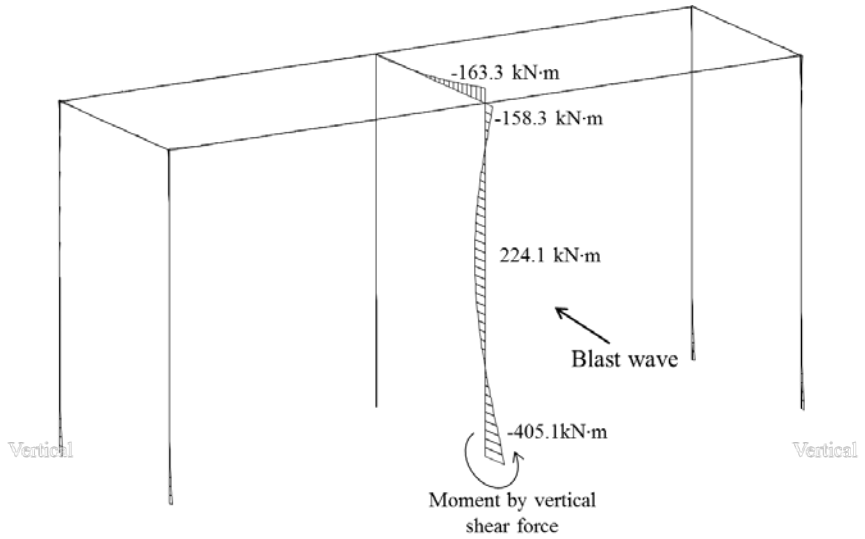

(b) Load case B

Figure 4-6 Shear force diagram

Table 4-3 Maximum shear force of columns and beams (kN)

Method	Load case	Column		Beam	
		Fixed	Hinged	Fixed	Hinged
TNT EM	Case A	-150.2	-270.4	(-) 41.3	(-) 24.5
	Case B	-325.8	-584.5	-93.9	-89
TNO MEM	Case A	-31.1	-47.6	(-) 9.8	(-) 5.3
	Case B	-51.1	-91.7	-15.9	-14.8
BST method	Case A	-94.4	-170.1	(-) 30.0	(-) 19.3
	Case B	-212.9	-381.8	-60.2	-57.3

The ratio of shear force is about 5:1:4 or 6:1:4 in Load case A or B, respectively. It is also quite similar to the ratio of required dynamic pressure.

4.3.5 Moment

Direction of moment is analyzed based on that of shear force (**Figure 4-7**). The analysis of moment is similar to that of shear force. The bending moment also is concentrated on the middle of the unit structure (**Figure 4-8**). The bending moment diagram (BMD) is symmetrically drawn based on the centerline of the front wall. Moment increases while closing the ends of columns or beams.

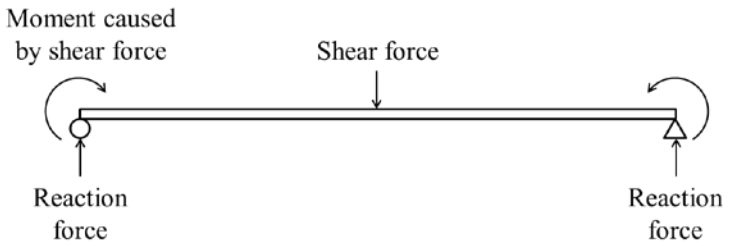

Figure 4-7 Moment caused shear force

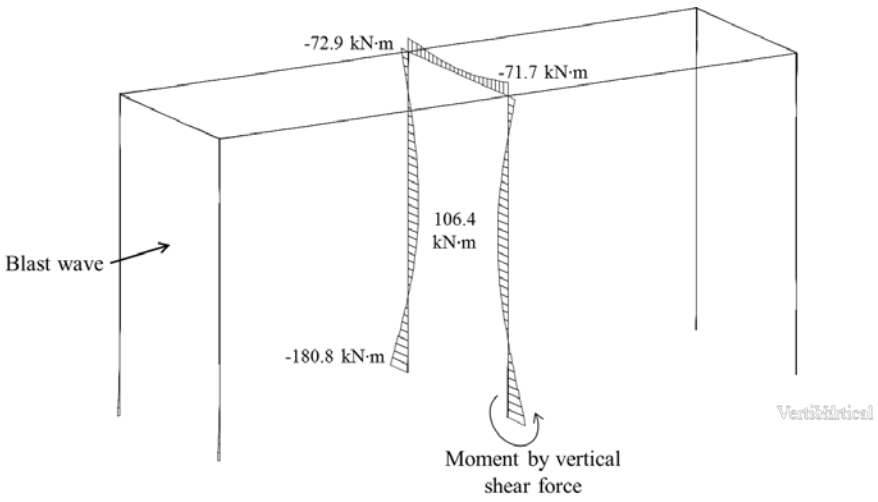

(a) Load case A

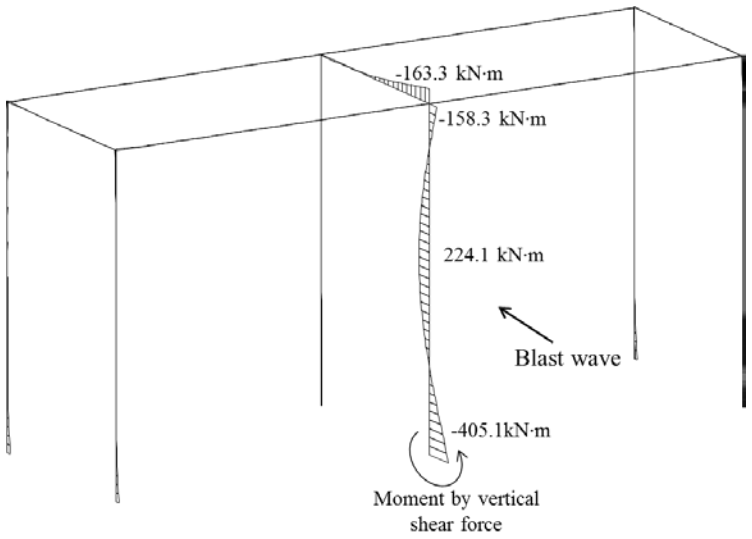

(b) Load case B

Figure 4-8 Bending moment diagram

Moments acting on columns are larger when they are caused by vertical shear force to the wall. When columns are included in the front (or rear) wall and side walls, moment by vertical shear force to the front (or rear) wall is larger. When the boundary condition is changed from the fixed to the hinged ends, the applied moment generally increases. The maximum moment of all

methods increases about 40% for hinged ends

As with shear force, maximum moment acting on beams is applied to the middle beam of the roof. The ends of beams have larger moment than the middle of beams. The middle beam of the roof experiences negative moment. When the boundary condition is changed from fixed to hinged ends, moment of members increases. Maximum shear force decreases with changed ends, but maximum moment increases with the changed boundary condition. The maximum moments of columns and beams are summarized in **Table 4-4**. In BMD of a simple beam, the positive moment is generally drawn in bottom of the beam. Similarly, the moment inside or outside of walls had the positive or negative sign. Because of the symmetric BMD, maximum beam moment acts in both negative and positive directions. In this case, the sign (-) means two opposite signs.

Table 4-4 Maximum moment of columns and beams (kN·m)

Method	Load case	Column		Beam	
		Fixed	Hinged	Fixed	Hinged
TNT EM	Load case A	-150.2	-270.4	(-) 41.3	(-) 24.5
	Load case B	-325.8	-584.5	-93.9	-89
TNO MEM	Load case A	-31.1	-47.6	(-) 9.8	(-) 5.3
	Load case B	-51.1	-91.7	-15.9	-14.8
BST method	Load case A	-94.4	-170.1	(-) 30.0	(-) 19.3
	Load case B	-212.9	-381.8	-60.2	-57.3

Also, the ratio of moment is similar to the ratio of required dynamic pressure; about 5:1:4 or 6:1:4 in Load case A or B, respectively.

4.3.6 Deformation

Deflection of the model is symmetric to the center of the front wall. Front and side walls are deformed inside the structure, in the same direction as the blast

load. The roof is deflected against the blast load (**Figure 4-9**). The cause of this is guessed to be the blast load on the front and side walls and too narrow area of roof . If the area of roof are larger, deflection to the direction of gravity would occur. The deformation occurs in largest walls like shear force and moment, concentrating on largest walls. Maximum deflection is on the largest walls even when blast waves are applied from the side, in Load case A. Deflection on the front wall is smaller to that of side walls. It is guessed that maximum deflection on side walls in Load case A is caused by the largest area. When the boundary condition is changed from the fixed to the hinged ends, the deflection of the model generally increases. The maximum moments of all methods increase about 86% for hinged ends.

The deformed shape of the roof is depending on boundary condition. When walls are connected with fixed ends, deformation of side walls is similar to lateral drift caused by front wave. In other cases which are Load case A and B with hinged ends, side walls are deflected inside, in the same direction of blast load. The different deformation shape of fixed ends on Load case B might be caused by narrow shape of the side walls. The rear walls with fixed or hinged ends tilt forward outside the structure. Maximum deflections caused by each method are summarized in **Table 4-5**.

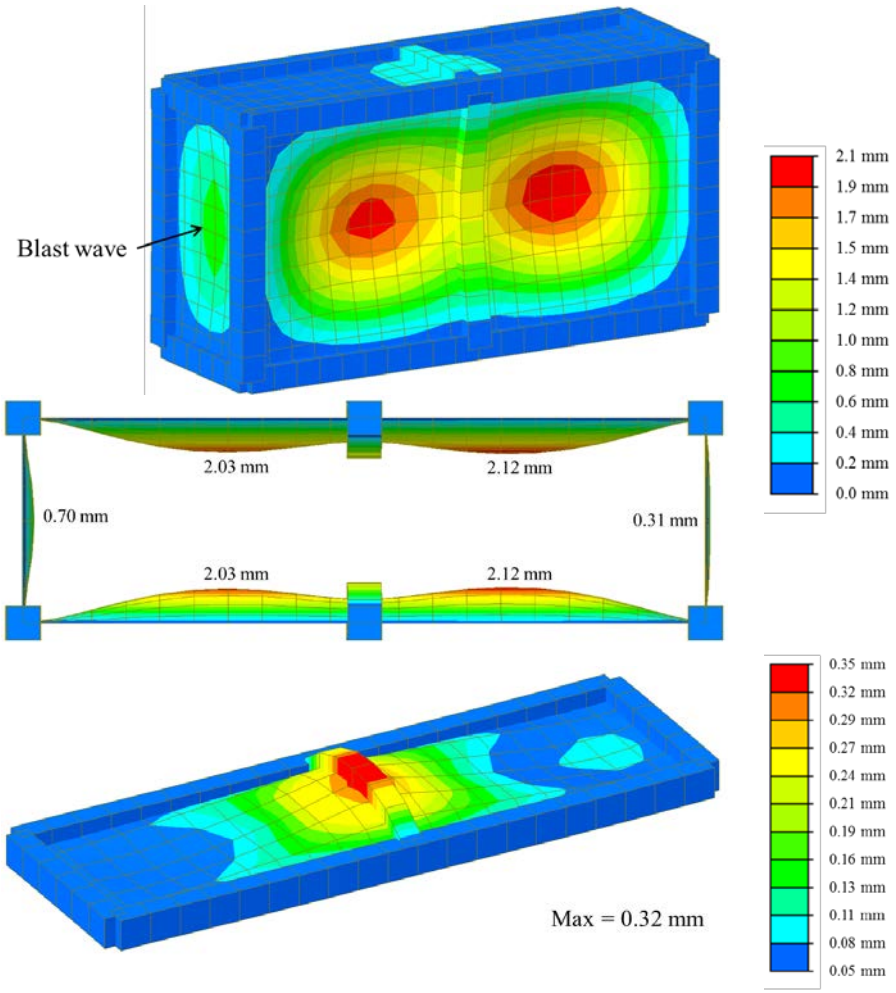
Blast wave
2.1 mm
1.9 mm
1.7 mm
1.5 mm
1.4 mm
1.2 mm
1.0 mm
0.8 mm
0.6 mm
0.4 mm
0.2 mm
0.0 mm
2.03 mm
2.12 mm
0.70 mm
0.31 mm
2.03 mm
2.12 mm
0.35 mm
0.32 mm
0.29 mm
0.27 mm
0.24 mm
0.21 mm
0.19 mm
0.16 mm
0.13 mm
0.11 mm
0.08 mm
0.05 mm
Max = 0.32 mm

(a) Load case A

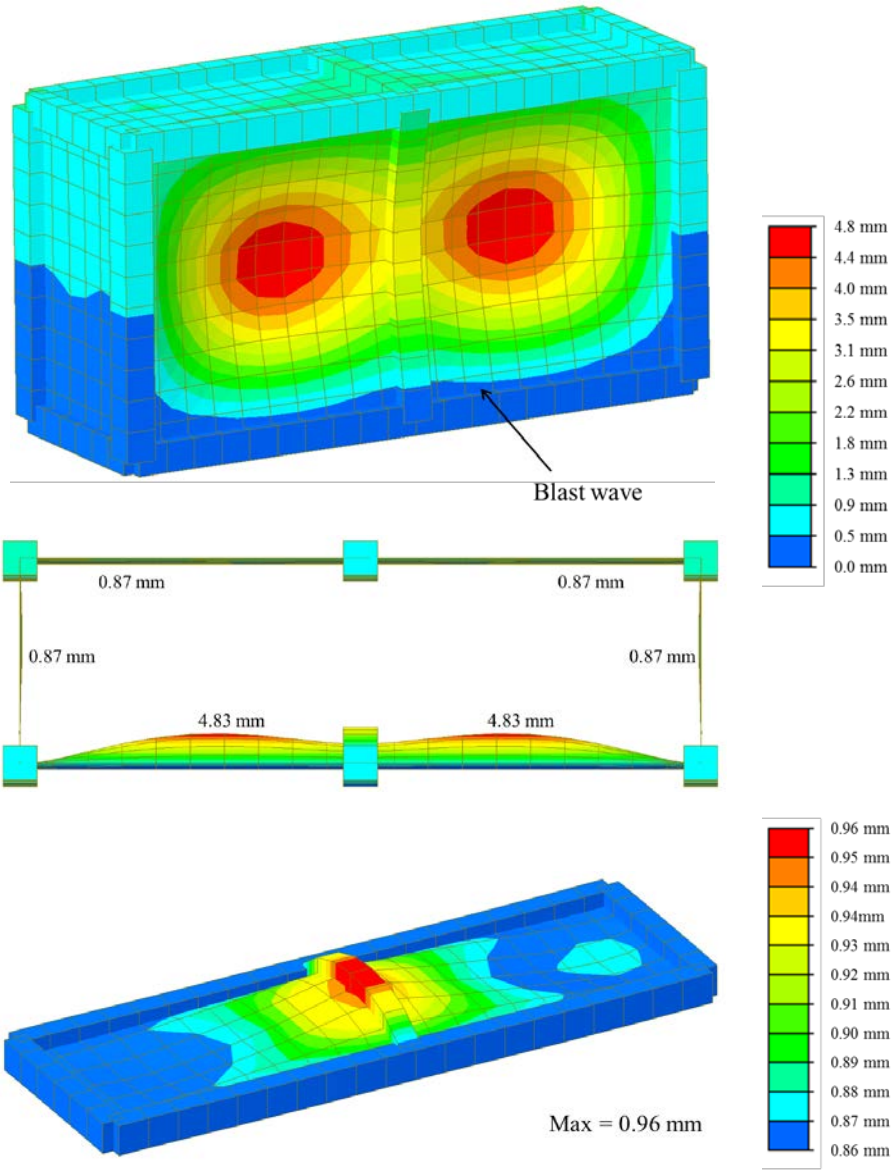

(b) Load case B

Figure 4-9 Deformation of model

Table 4-5 Maximum deformation (mm)

Method	Load case	Maximum deformation	
		Fixed	Hinged
TNT EM	Load case A	2.12	3.97
	Load case B	4.83	8.89
TNO MEM	Load case A	0.37	0.70
	Load case B	0.76	1.40
BST method	Load case A	1.33	2.48
	Load case B	3.16	5.81

The ratio of deformations among three methods is 6:1:4. It is similar to the ratio of required dynamic pressure, as well.

4.4 Comparative dynamic analysis for wall design check

4.4.1 Equivalent SDOF system of unit model

In blast resistant design, the structure is analyzed based on member by member approach. Structural response parameters of members are used for design check: ductility ratio, μ, and support rotation, θ (ASCE, 2010; Dusenberry, 2010). When the maximum displacement of the member is divided by the displacement at the elastic limit, it is called ductility ratio, μ. Hinge rotation is related to maximum deflection of span. The symbol, θ, is defined in two ways (**Figure 4-10**): rotation at support or middle of span. Because support rotation is referred in response limit, member design is also checked based on support rotation. Limitations are various depending on the material, structural type, structural member and protection level. The criteria suggested by ASCE (2010) is used here, but there are other limitations suggested by UFC or DoD (Departure of Defense) (Dusenberry, 2010).

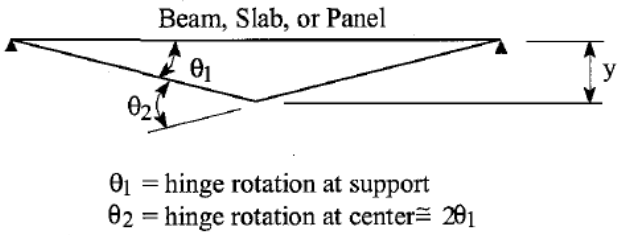

Figure 4-10 Hinge rotation (ASCE, 2010)

The maximum deflection related to response parameters is the response of equivalent SDOF building while most buildings have multi-degree-of-freedom (MDOF). Because analysis of a MDOF building requires complex computations, MDOF buildings, for convenience, are converted to SDOF buildings. The response parameters, ductility ratio and support rotation are also responses of the equivalent SDOF building.

Because the structural responses are based on the equivalent SDOF system, computing the equivalent SDOF system is the first step. Variables of SDOF buildings are calculated with transformation factors. The transformation factors for common one way or two way structural members are summarized in Biggs (1964) or UFC (2008). Transformation factors are selected for computing equivalent variables: mass, stiffness, force or resistance. These factors for one or two way members are dependent on loading diagrams, boundary conditions, and strain ranges. For different loading conditions, three loading diagrams are suggested: distributed, one or two pointed load. Three boundary conditions are considered: simply supported, fixed end and simply-fixed boundary conditions. Elastic and plastic strain ranges are considered. Elasto-plastic range is included or not. More details are explained in Biggs (1964) and UFC (2008).

Natural period of equivalent SDOF system, which is one of the main variables for dynamic analysis, can be computed with equivalent mass and stiffness. The equivalent mass or stiffness is computed by multiplying transformation

factor to mass, K_M, or stiffness, K_L. For convenience, the single load-mass transformation factor, K_{LM}, is used. The mass transformation factor, K_M, divided by load transformation factor, K_L, is single load-mass transformation factor, K_{LM}. Based on the equation of motion, the equivalent mass is computed by multiplying single load-mass transformation factor, K_{LM}, and the stiffness member is used instead of equivalent stiffness. The stiffness of members is calculated by elastic modulus, moment of inertia and length of member, and is dependent on boundary conditions. With the same equation (EI/L^3), a different constant is multiplied for considering different boundary conditions. Moment of inertia changes in accordance with the section condition. If the member is cracked or failed, the moment of inertia is also changed. The average of gross and cracked moment of inertia is used for considering the section cracked by blast load. Once equivalent mass and stiffness are obtained, natural period of the building is obtained by **Eq. (4-4)**.

$$t_n = \sqrt{\frac{M_{eq}}{K_{eq}}}, \quad K_{eq} = n\frac{EI_{avg}}{L^3} \tag{4-4}$$

Where,

n	:	constant depending on loading and boundary conditions
M_{eq}	:	equivalent mass of the member
K_{eq}	:	equivalent stiffness of the member
I_{avg}	:	average moment of inertia = (I_{gross}+$I_{cracked}$)/2
I_{gross}	:	moment of inertia of gross area
$I_{cracked}$	:	moment of inertia of cracked area
E	:	elastic modulus of material
L	:	length of member

4.4.2 Wall design check

Blast resistant design can be checked by hand. Walls are evaluated based on three empirical methods of the gas explosion. Response parameters, ductility ratio and support angle are computed and then checked in accordance with response criteria (ASCE, 2010).

Design check processes are different depending on types of structural members. Because the main purpose is to compare ductility ratio and support angle under different gas explosion methods, only the front wall is checked. When checking the wall design, side walls are analyzed only to check the interaction of in-plane and out-of-plane shear wall forces. The process for the blast resistant wall design check is shown below:

(1) Compute the reflected overpressure, P_r, and equivalent duration, t_e, referred to the peak overpressure, P_{SO}, and duration, t_d.

(2) Determine blast resistance of member, R_u, the smaller value between dynamic bending and shear resistance.

(3) Compute member properties of equivalent SDOF system: average moment of inertia, equivalent stiffness, equivalent mass and natural periods.

(4) Determine elastic deflection, y_e.

(5) Determine ductility ratio.

(6) Compute maximum deflection, y_{max}, and then support rotation.

(7) Check the ductility ratio, μ, and support rotation, θ, in accordance with response criteria.

For dynamic bending and shear resistance of members, dynamic material properties should be considered. Blast resistant design in onshore industry, strength increase factor (SIF) and dynamic increase factor (DIF) are used.

More details about the two increase factors, SIF and DIF, are explained below in Section 4.5.4. As compared with dynamic bending and shear resistance, lower dynamic resistance is used.

The properties of equivalent SDOF system could be computed in Section 4.4.1. Moment of inertia is an average value of gross and cracked moment of inertia. Transformation factor of mass is the average of elastic and plastic single load-mass factors, K_{LM}. With these equivalent values, the equivalent natural period is obtained by **Eq. (4-4)**. As maximum member resistance is divided by stiffness of member, it is elastic deflection.

The ductility ratio can be determined based on the graphic solution methods. Graphic solution methods suggest charts, which are solutions of dynamic equilibrium equations and available in Biggs (1964) and UFC (2008). Users can read off ductility ratio with maximum resistance, blast load, blast loading duration and natural period. The support rotation could be computed with maximum deflection based on the obtained ductility ratio. The graphical chart for elasto-plastic SDOF system is used (**Figure 4-9**). Two ratios are needed to determine ductility ratio and loading duration to natural period. The maximum force, F_0, takes the reflected overpressure on front walls and it is different from the equivalent blast load used in modeling. The other values are explained above.

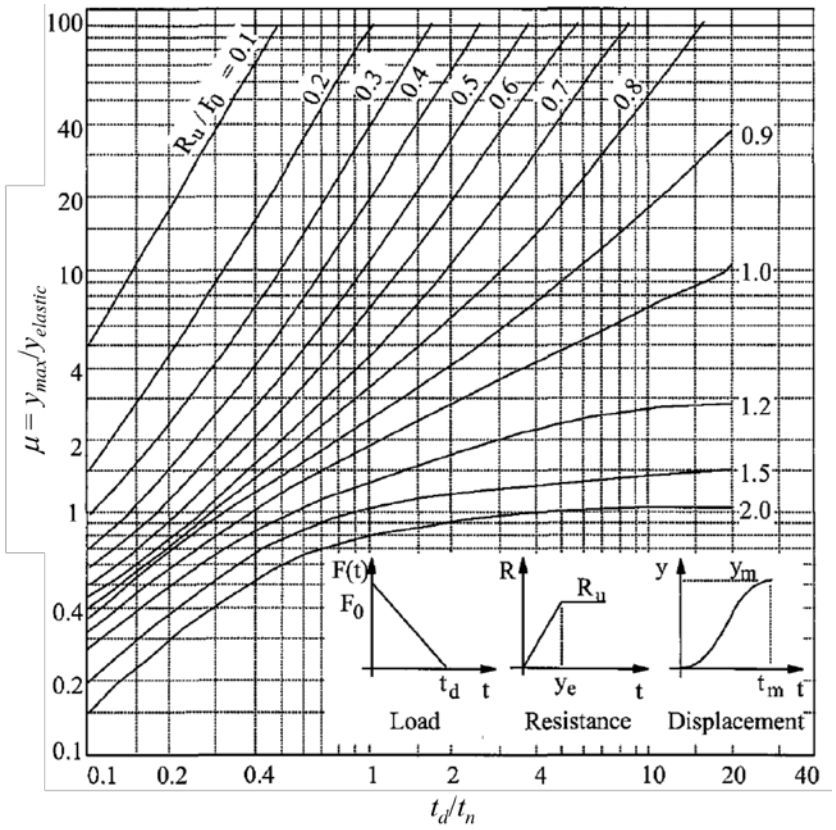

Figure 4-11 Graphic solution chart for equivalent SDOF system (ASCE, 2010)

For maximum deflection, elastic deflection is multiplied by ductility ratio, which is read off in **Figure 4-11**. Based on a trigonometrical function, support angle, θ, could be computed by **Eq. (4-5)**

$$\theta = \tan^{-1}\left(\frac{y_m}{0.5L}\right) \tag{4-5}$$

Wall design conditions in this thesis are explained as the following. The wall is designed referred to an existing blast resistant wall design applied to real plant structures. The re-bar of diameter 12 mm (ϕ12) is placed per 125 mm. Thickness of wall and length of member follow those of a unit model, 200 mm and 5000 mm, respectively. Because blast load is applied as pressure load, loading diagram for distributed load is considered. Walls of the unit model have fixed or simply-fixed boundary conditions as explained above. Boundary conditions change during construction and construction conditions of walls is especially uncertain. Simple supported boundary condition is considered for worst cases. For economical design, elasto-plastic range is considered. Transformations factors are the average of elastic and plastic factors. The elastic load and mass transformation factors are 0.64 and 0.5, respectively. The plastic load and mass transformation factors are 0.5 and 0.33. The equivalent mass of concrete is multiplied by the average single load-mass transformation factor. Because stiffness is zero in plastic range, elastic stiffness is used. In calculating stiffness, 385 is applied to constant ($385EI_{avg}/L^3$). The calculated maximum resistance and natural period of the unit wall are 112.42 kN and 0.11 sec, respectively. Ductility ratio and support angle are computed per each empirical method. They are summarized in **Table 4-6**.

Table 4-6 Maximum force, loading duration and response parameters

Method	P_r (kPa)	t_e (sec)	μ	θ (°)
TNT EM	100.55	0.05	10.5	5.1
TNO MEM	11.0	0.14	0.82	0.4
BST method	40.1	0.22	25.2	11.5

If a gas explosion is predicted by TNT EM, this wall design is not accepted in accordance with ductility ratio. As wall design is judged by support rotation: however, it is dependent on building damage levels; Low, Medium and High. Each building damage level requires different support rotation and this design

can be accepted in high response. It is guessed this wall design can be accepted or not following engineer's judgement. Under the gas explosion estimated by the TNO multi-energy method, the wall design is also accepted in accordance with ductility ratio, μ, and support rotation, θ. It satisfies the limits of all building damage levels. The ductility ratio and support rotation predicted by the BST method are too large due to the two reasons that the reflected overpressure is large and that the duration, t_d, is large with respect to the natural period (see **Figure 4-11**). Because the equivalent loading duration is two times the natural period, resonance cannot be a cause. As referred to in Section 3.3, duration predicted by the BST method shows unordinary tendency. Because the BST method does not give any graphs for duration of gas explosion, the duration estimated by BST method could be inaccurate. It is guessed that this inaccurate duration can contribute to these abnormal results.

The ductility ratio or support angle is not proportional to input overpressure, unlike structural behavior. Results of structural behavior follow the maximum member resistance, which is a static blast load. Large or small blast loads cause large or small deformation, of course. It is unsure which method gives more proper or applicable results but it is carefully recommended that the BST method is not used to check structural responses.

4.5 Connection design

4.5.1 Schematic design

Precast concrete (PC) connections are used in various joints, but the following section primarily deals with the connections between walls and ground beams. The welded headed studs, mainly used for wall bottom connections, require welding in the field (**Figure 4-12**).

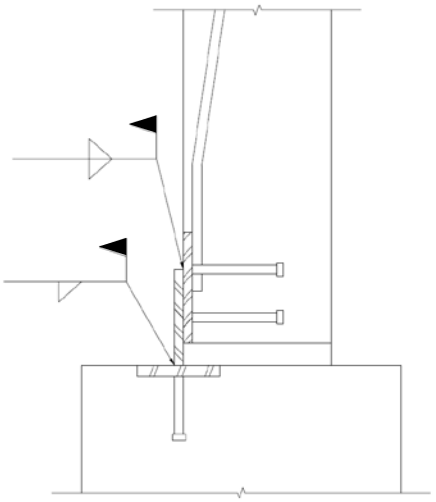

Figure 4-12 General PC wall connection (PCI, 2008)

In order to increase workability, the other connection design using angles and anchor bolts is used in this section. Forces on PC walls move at an angle via the plate, welded at an angle and installed in a PC panel cover. Re-bars, so called tails, are welded on the plate for reinforcement and for integration of the plates (**Figure 4-13**). Since the blast loads are determined based on three various gas explosive methods, the varying capacity numbers suggest that comparisons on the basis of a single design would be more efficient.

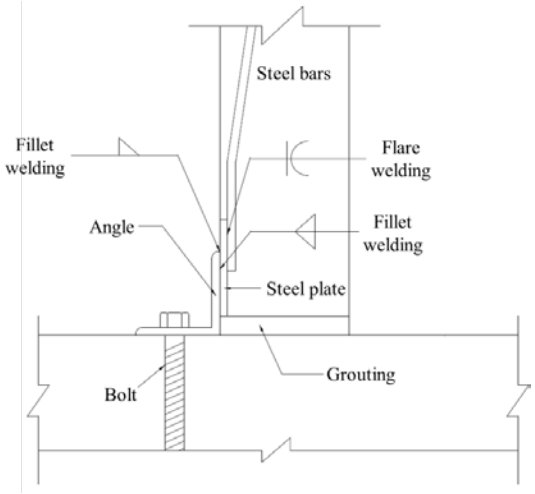

Figure 4-13 Suggested PC wall connection

4.5.2 Design force

Three types of forces are considered when designing the connections: both the vertical and horizontal forces to the walls (V_n and H_n) as well as the tensile force (T_n) on bolts (**Figure 4-14**). The applied axial forces are used only to determine the strength of panels and foundation concrete since these connections are installed in the bottom of the PC panels.

The required shear forces are easily obtained through the results of the structural analysis program, while the tensile forces acting on bolts require calculating. The way to achieve this is through a mechanical approach using a free body diagram (FBD) in regards to connections (**Figure 4-15**).

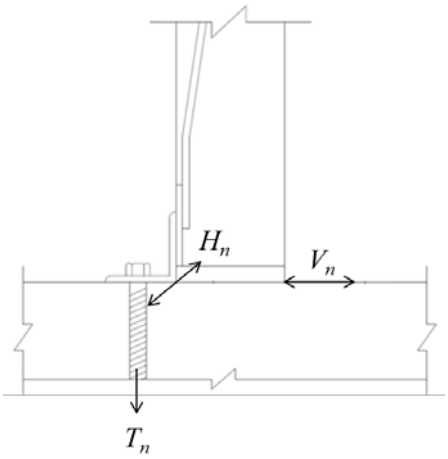

Figure 4-14 Forces for design of connection

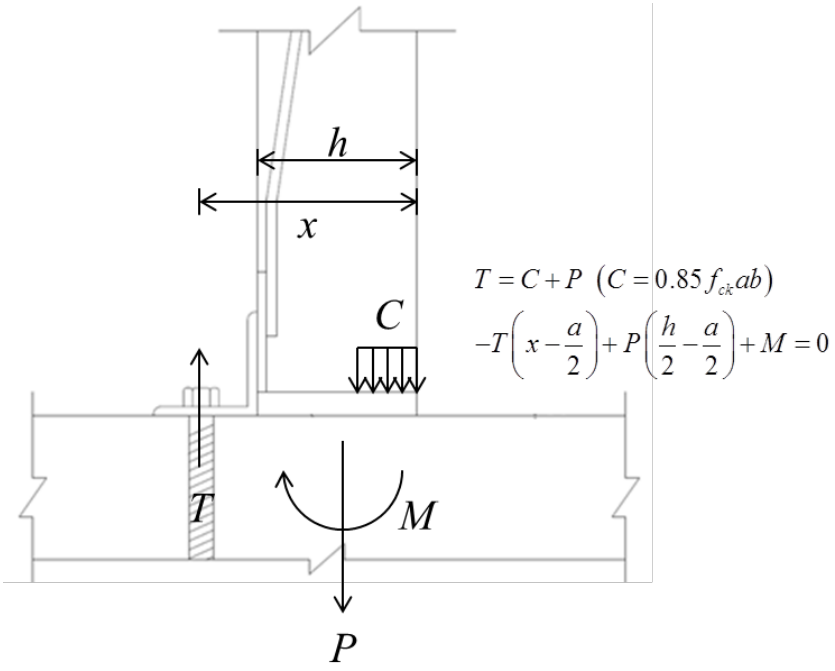

Figure 4-15 FBD for tensile force

Tensile force applied to inserted bolts can be obtained by equations suggested by PCI (2004) but those equations are not available in this case. Inserted bolts suggested by PCI (2004) are subjected only to tensile force. This connection, however, is the applied combination of the axial force and shear force. The

mechanical approach is the only way for tensile force on bolts. After depth of compression, *a*, is computed, tensile force can be obtained.

4.5.3 Design condition

The material commonly used for connections is metal including the angles, bolts, plates, re-bar, and base metals. The static properties of elements are based on ASTM and the sizes cited here are in reference of the PCI design handbook (2004) and the Steel Construction Manual 14th edition (AISC, 2011). The materials used for the angles, bolts, and plates are ASTM A36, ASTM A193, and SM490, respectively. Different welding techniques are required for angles and plates. In particular, fillet welding is carried out between angles and plates. Flare welding, on the other hand, is required for re-bar. The base metal has 550 MPa of yield strength.

Concrete is used for the foundation and PC panels. Concrete usually is classified by compressive strength, which is estimated after passing 28 days since placing, f_{ck}. The strength of the foundation concrete is 28 MPa. PC concrete and PC panels are 34 MPa.

The size of all of the elements are determined by the PCI design handbook (2004) and the Steel Construction Manual 14th edition (AISC, 2011). The angles has legs of 130 mm, a thickness of 23 mm, and a length of 180 mm. two bolts have diameter of 22 mm, an embedded length of 250 mm and distance between bolts is 80 mm. The plates had a length of 230 mm, a height of 200 mm, and a thickness of 25 mm. The re-bar used as tails has a diameter of 190 mm (DB19) and a welding length of 130 mm on the plate.

4.5.4 Dynamic properties of materials

Generally material strength increases under dynamic loads. Practically installed steel shows a strength increase of twenty five percent (ASCE, 2010). The strength increase factor (SIF) is suggested to consider a material's increased strength. Each material has a different SIF and these are

summarized in **Table 4-7** (UFC 3-340-02, 2008). The SIF is usually ignored in design of nuclear plants. However, petroleum plants on the other hand are typically designed with consideration of the SIF.

Table 4-7 Strength increase factor (SIF) per material (ASCE, 2010)

Material	SIF
Structural steel ($F_y \leq$ 345 MPa)	1.1
Reinforcing steel ($f_y \leq$ 414 MPa)	1.1
Cold-formed steel	1.21
Concrete	1.0

When loading increases at a quick pace, structures don't have enough time to react to the increased load. This results in an increase in the yield strength and a decrease in the ductility of members. This phenomenon is commonly known as the dynamic increase factor (DIF). A DIF is dependent on the types of material and forces involved (**Tables 4-8** and **4-9**). Each type of force and material requires a different reaction time against the loading.

Table 4-8 Dynamic increase factors (DIF) for reinforcing bars, concrete and masonry (ASCE, 2010)

Stress type	DIF			
	Reinforcing bars		Concrete	Masonry
	f_{dy}/f_y	f_{du}/f_u	f'_{dc}/f'_c	f'_{dm}/f'_m
Flexure	1.17	1.05	1.19	1.19
Compression	1.10	1.00	1.12	1.12
Diagonal tension	1.00	1.00	1.00	1.00
Direct shear	1.10	1.00	1.10	1.00
Bond	1.17	1.05	1.00	1.00

Note: f_{dv} is the dynamic yield strength of steel bars; f_{du} is the dynamic ultimate strength of steel bars; f'_{dc} is the dynamic compressive strength of concrete and f'_{dm} is the dynamic strength of masonry

Table 4-9 Dynamic increase factors (DIF) for structural steel, cold-formed steel and aluminum (ASCE, 2010)

Material	DIF		
	Yield stress		Ultimate stress
	Bending/Shear	Tension/Compression	
	F_{dy}/F_y	F_{dy}/F_y	F'_{dc}/F'_c
ASTM A36	1.29	1.19	1.10
ASTM A588	1.19	1.12	1.05
ASTM A514	1.09	1.05	1.00
ASTM A653	1.10	1.10	1.00
SAE AMS5501 (stainless steel)	1.18	1.15	1.00
SAE AMS4113 (aluminum)	1.02	1.00	1.00

In blast resistant designs, the properties of materials are considered by multiplying the SIF and the DIF to static properties, **Eq. (4-6)**.

$$F_{dy} = \text{SIF} \times \text{DIF} \times F_y \quad \text{or}$$
$$F_{du} = \text{SIF} \times \text{DIF} \times F_u \qquad (4\text{-}6)$$

Where,

F_{dy} : dynamic yield strength
F_{du} : dynamic ultimate strength
SIF : strength increase factor
DIF : dynamic increase factor

The two strength increase factors, SIF and DIF, are chosen based on whether the materials are included in tables like the basic material of welding and whether or not the two strength increase factors are in unity.

4.5.5 Applied force

The applied forces are determined based on results of the FEA program, MIDAS Gen. Because the suggested PC connections are located in bottom of walls, reaction forces at bottom are considered to affect the capacity of connections. As the front, side or rear walls are proposed to be applied distributed force, pointed reaction forces at every bottom nodes are converted to distributed forces. The tensile force is calculated as explained in Section **4.5.2**. As done in structural member design, maximum reaction forces are considered for design. It is judged the front wall endures maximum forces and requires maximum number of connections when blast waves progress in Z-direction. The maximum reaction forces caused by TNT EQ, TNO MEM, and BST method are summarized in **Table 4-10**. Because the sign of forces is less important in design, the absolute values are only used. The moment on tables meant longitudinal moment of bottom beams. In the table, the reacted vertical shear force, horizontal force and tensile force to walls are marked as V_n, H_n and T_n, respectively.

Table 4-10 Reacted shear and tensile forces

Force per length	Method	Boundary condition	
		Fixed ends	Hinged ends
V_n (kN/m)	TNT EQ	183.8	200.4
	TNO MEM	28.9	25.7
	BST method	119.7	106.9
H_n (kN/m)	TNT EQ	19.1	32.5
	TNO MEM	2.9	5.0
	BST method	12.6	21.3
T_n (kN/m)	TNT EQ	164.8	206.6
	TNO MEM	28.2	31.7
	BST method	121.4	135.7

As analyzed above, reacted vertical shear force is larger than horizontal shear force. By Newton's Law, larger shear force results in larger reacted force. Similarly, shear and tensile forces applied to connections increase as boundary condition is changed from fixed to hinged ends. The ratio of forces between methods is slightly different with structural behaviors. Reaction force predicted by TNT EQ is estimated as larger than the other methods. Reaction force by TNT EQ is from six to eight times more than TNO MEM (6:1:4, 7:1:4 or 8:1:4).

4.6 Capacity of connection under blast load

Plates and re-bars are buried in concrete panels, causing integrity with concrete. Since their capacities are determined by the concrete, no additional considerations for capacities are needed.

4.6.1 Angle

The vertical shear force, perpendicular to the longitudinal direction of angles and marked as V_u in **Figure 4-10**, is obtained by the PCI (2004) suggestion, **Eq. (4-7)**. The eccentricity, e_v, is calculated with the assumption that the shear force is applied at the middle height of the plates. From the bottom of the angles, the thickness of the grouting and the half of the plates are summed. The horizontal shear force, parallel to the longitudinal direction of the angles and marked as H_u in **Figure 4-10**, is obtained by the AISC (2010) suggestions, **Eq. (4-8)**.

In order to check the angle capacity, axial forces acting on angles are considered as suggested by PCI (2004). This axial load is marked as N_u in **Figure 4-13 (b)** and obtained by **Eq. (4-9)**.

$$V_{dn} = \frac{F_{dy} b_n t^2}{4e_v} \tag{4-7}$$

Where,

V_{dn} : dynamic shear capacity (in vertical direction)
F_{dy} : dynamic yield strength of steel
b_n : (length of angle)-(hole diameter)-1.59 mm
t thickness of angle

$$H_{dn} = 0.6F_{dy}A_wC_v = 0.6F_{dy}\left(bt\right)C_v \tag{4-8}$$

Where,

H_{dn} : dynamic shear capacity (in horizontal direction), kN
F_{dy} : dynamic yield strength of steel, kN
A_w : effective area of welding, mm^2
b leg length of angle, mm
C_v : lag shear coefficient

$$N_{dn} = \frac{F_{dy} t^2 b_n}{4g} \geq N_{du} \tag{4-9}$$

The lag shear coefficient, C_v, could be obtained by three cases. The shear coefficient determined as 1.0 in this case.

$$b/t \leq 1.10\sqrt{k_v \frac{E}{F_y}} \tag{4-10}$$

Where,

b : width of the leg, mm
t : thickness of angle, mm
k_v : 1.2

4.6.2 Bolt capacity

Bolts used for connections directly resist the shear forces, V_n and H_n. This means that bolts require checking for their capacity of shear forces. The shear capacity is obtained by **Eq. (4-11)**, as suggested by AISC(2010).

Bolts against tensile forces react in the case of shear forces. The tensile capacity is obtained by a similar equation, **Eq. (4-12)**.

These bolts are one of a kind anchor rods, which require the breakout and pullout strength of concrete. Bolts, in this case, are assumed to be long enough that they would not pull out. The dynamic breakout strength of the foundation concrete, N_{dcb}, is obtained by **Eq. (4-13)**, following PCI (2004). The projected surface area, A_N, is various depending on location of the stud group. Because the bolts group is installed in foundation, the proper equation for A_N is chosen.

$$V_{dn} = H_{dn} = nF_{duv} \tag{4-11}$$

Where,

n : number of bolts
F_{duv} : dynamic required strength of bolts, kN

$$T_{dn} = nF_{dut} \tag{4-12}$$

Where,

T_{dn} : designed dynamic tensile strength of bolts, kN
F_{dut} : dynamic ultimate strength of bolts, kN

$$N_{dcb} = C_{bs} A_N C_{crb} \Psi_{ed,N} = C_{bs} (X + 3h_{ef})(Y + 3h_{ef}) C_{crb} \qquad (4\text{-}13)$$

Where,

N_{dcb}	:	dynamic nominal concreate break strength
C_{bs}		break out strength coefficient,
A_N	:	projected surface area for a stud/bolt or group of studs/bolts
C_{crb}	:	cracking coefficient of breakout, 1.0 or 0.8
$\Psi_{ed,N}$	:	edge distance factor
h_{ef}	:	effective embedment depth
X	:	distance between bolts in X-direction
Y	:	distance between bolts in Y-direction

4.6.3 Welding

There are two welded parts: the plates with angles and the re-bar on plates. Fillet welding, which is common in steel construction, is used when plates are welded with angles. Re-bar welded onto plates require flare welding. These two types of welding resist shear forces caused by load. The shear capacity of welding is obtained by **Eq. (4-14)**. The shear capacity of welding depends on the strength of the base metal, geometric conditions related to the welding, and the effective area of the welding.

The capacity for welding is affected by the strength of the base metal. The strength is usually 345 MPa, and this factors unity. AISC suggests that a large factor determining the strength of a base metal is the parent metal. The AISC suggests 1.03 when the strength of the base metal is 551 MPa (80 ksi).

The strength of welding also increases the geographic conditions of the welding including the shape of the welding and its eccentricity. The suggested connections have C shaped welding, and forces are not loaded at the center of gravity in the weld group. The PCI suggests three methods to consider the effect of weld group: the mechanical relationship between the weld group and the load, numerical analysis, and tabulated value suggested by the AISC (2010). The method suggested by the AISC (2010) is selected here. For the channel shaped welding, the value is determined as 3.152.

The effective area of welding, marked as A_w in **Eq. (4-14)**, is calculated by multiplying a factor with the thickness of the welding. The factor depends on the welding type, which means fillet and flare welding have different effective thickness. In the case of fillet welding, 0.7 is multiplied to the thickness, and 0.3 is multiplied to the diameter of re-bar in the case of flare welding (AWS, 2010).

$$V_{dn} = 0.6CC_1F_{EXX}A_w \qquad (4\text{-}14)$$

Where,

C : coefficient for concentrically loaded weld group, kN
C_1 electrode strength coefficient
F_{EXX} : strength of base metal, kN

4.6.4 Total capacity of connection

Based on equations explained above, the capacity of one connection is summarized below (**Table 4-11**). The minimum capacity for each force determines the total capacity of the connection. The number of connections is checked based on the minimum values. These values are bold.

Table 4-11 Capacity of material

Member		V_n (kN)	H_n (kN)	T_n (kN)
Angle		**86.2**	596.5	-
Bolt		**231.2**		414.0
Foundation		-		**284.4**
Welding	Fillet	770.7	2502.3	913.2
	Flare	502.5	646.9	502.5

Because the tensile force applied on angle could not occur by blast load, the tensile capacity of angles is neglected. In connection design, the tensile capacity of concrete is considered because of the breakout capacity. If the welding fails, the performance connections would not be perfect. Welding capacities of shear forces and the tensile force are also considered.

4.6.5 Required number of connection

There are three methods are used to predict the blast load. For convenience, the capacity of suggested connection is used to determine the number of connection. The blast load caused by each method is compared with the number of connection. The needed number of connection is summarized in **Table 4-12**.

Table 4-12 Required number of connection

Type of method	Required force per length	Required connection number	
		Number per length (EA/m)	Total number (EA)
TNT EQ	V_n (kN/m)	**3**	78
	H_n (kN/m)	1	
	T_n (kN/m)		
TNO MEM	V_n (kN/m)	**1**	26
	H_n (kN/m)		
	T_n (kN/m)		
BST method	V_n (kN/m)	**2**	52
	H_n (kN/m)	1	
	T_n (kN/m)		

Note: Bold numbers mean the total number per

Because the number is the same in fixed or hinged ends, there is no division following boundary conditions. Following the data in **Table 4-12**, the vertical shear force to walls determines the number of connection. The ratio of required connection number is 3:1:2. This ratio is smaller than the ratio of response of structures or the equivalent static blast load. This ratio can create a misunderstanding; there is little difference between methods but the total connection number shows a large gap. If this ratio is applied to real buildings, the total quantities per method are quite different.

Chapter 5. Conclusion

In this research, the gas explosive models are researched and the typical three methods included in the empirical model are mainly compared. The comparative analysis of three gas explosive empirical methods is carried out firstly. Then, the different results are researched and compared when they are applied on the scenario-based blast resistant design: the blast load, structural behaviors, the design check, and the blast resistant design of PC panel connection.

5.1 Gas explosion model

In the **Chapter 2**, various models used to predict the results of a gas explosion are researched. The findings are summarized below:

1) Damages of the gas explosion are depending on various factors. Geographical conditions especially determine the results: the density, size, shape and arrangement obstacle, and the degree of venting. Gas explosion models are suggested to precisely predict results.

2) Gas explosion models are divided in three: the empirical model, the semi-empirical model, and the computational fluid dynamic (CFD). The empirical model is based on the large amount of experiments and used in onshore industry. The CFD is based on solutions of fluid movement and used on offshore industry. The main focus of this research is on the empirical model.

3) The TNT equivalency method is simple to use and widely used in blast resistant design but not recommended in case of gas explosion. The alternatives are suggested and TNO multi-energy method and

Baker-Strehlow-Tang (BST) method are mostly popular in onshore industry. The TNO multi-energy method and the BST method use the class number and Mach number for considering various geographical conditions, respectively. For accurate predictions, the owner or engineers choose the proper number, and it leaves lack of objectivity.

5.2 Comparative analysis and different designs of three empirical methods

In **Chapter 3**, two studies are done. The existing guidelines practically used in the onshore field were based on the TNT equivalency method. Firstly, the corresponding class or Mach number of the existing guideline is researched. Then, comparative analyses of three empirical methods are carried out to show the different characteristics and results of methods. The several important observations and conclusions are summarized below:

1) The overpressure by the existing guideline – explosion corresponding to 1 ton of TNT far from 100 ft. – has the class number between 6 and 7 or the Mach number between 0.7 and 1.0. In the industrial field, these numbers are quite high. The possibility of high number explosions occurring is relatively low, so this could be guessed as the cause for the conservativeness of the existing guideline.

2) At the same distance, the TNO multi-energy and BST method provide various overpressure values because of the difference in the class and Mach number, respectively. Over certain numbers, the overpressure by the TNO multi-energy and BST method shows convergence instead of steady increase. If the overpressure of an explosion is measured at difference distances, the TNT equivalency method rapidly decreases. The TNT equivalency method predicts larger overpressure at close distances, but at far distances, it causes the lower overpressure than the TNO multi-energy and BST method.

It corresponds to the limitation of the TNT equivalency method (Lenoir and Davenport, 1993): too little overpressure at far distances. The overpressure by the TNO multi-energy and BST methods do not increase even at closer distances while TNT equivalency method shows non-linear increase of overpressure. The overpressures by gas explosions become stronger to a certain degree and then are maintained steadily. In case of hemispherical explosions, the overpressures are larger than those of spherical explosions. The Mach stem generated by the reflected overpressure is guessed to be the main reason.

3) With similar overpressure, the duration of the TNT equivalency method is surely shorter than other methods. If the class or Mach number is determined based on the duration, the corresponding class number or Mach number of the guideline would be between 5 and 6 or 0.35 and 0.7. The duration by the TNT equivalency and other methods has different tendency. The duration by the TNT equivalency method increases non-linearly with increasing distance. The duration by the TNO multi-energy and BST methods decreases and then increases depending on distance. Explosions with the higher class or Mach number are predicted to have shorter durations. In case of hemispherical explosions, durations become longer than those of spherical explosions.

4) The TNT equivalency and BST methods provide graphs for the impulse, but the TNO multi-energy method just suggests a calculation equation ($I_W = P_{SO} \times t_d/2$) based on the simplified triangular graph. The impulse of the TNT equivalency method provides a smaller impulse than the BST method even with similar overpressure and duration. The TNO multi-energy method gives significantly more conservative impulses than the BST method. Among the dynamic analysis methods, the P-I method of graphic solution methods

provide the pressure-impulse diagrams and checks structural damage level based on pressure and impulse. If a structure is estimated based on the P-I method, TNO MEM predicts more severe damage than by the TNT equivalency or BST method. In the case of hemispherical explosions, impulses are larger than those of spherical explosions. It may be caused by higher overpressure and longer duration of the hemispherical explosion.

In **Chapter 4**, these methods are applied on blast resistant design. In onshore industry, the overpressure and the blast load by gas explosions are assumed based on scenarios. One scenario is made referred to gas explosion books. After analysis of structural behaviors by blast loads, the wall deformations by three empirical methods are checked. Finally, a PC panel connection is used to research different results by three methods. The several findings and conclusions are summarized below:

1) The blast load applying on the structure is different depending on both the kind of empirical model and the loading direction. Reflected overpressure, P_r, applied to the front wall are over two times of the peak overpressure, P_{SO}. Effective overpressure, P_a, applied to side walls and roofs are similar to the overpressure. As plants of onshore industry are designed, the maximum resistance of member, R_m, is used as static blast load. With the same conditions, the ductility of a member affects the static blast load. As the ductility increases, the static blast becomes smaller, even under blast pressures applied on structural members.

2) Based on the scenario, the TNT equivalency method predicts the largest blast load and the TNO multi-energy method suggests the smallest overpressure. The ratio of overpressures by the TNT equivalency method, TNO multi-energy method and BST method is 8:1:3.5. The ratio of the equivalent static blast load is changed to

6:1:4. If the class or Mach number is changed, the overpressure, dynamic and static blast load are changed.

3) When the blast load is applied on the structure, columns on the front wall lift up. This may cause the increase of axial force of rear columns. Maximum shear force and moment concentrate on middle members in the largest walls. When blast load is applied in the structure, members are loaded inside and deflect inside except the roof. The roof is the only plate having the negative convex. It is guessed that this is caused by the short width of the structure. If the structure has enough span between the roof beams, the roof could have a positive convex. When PC panels are not fixed on beams perfectly, larger forces and moments are applied on members and deformations also increase.

4) In blast resistant design, the designs of members are checked with the ductility and/or the rotation angle at support. With the same PC panel, the wall is checked after conversion to the equivalent single-degree-of-freedom (SDOF) system. The ductility predicted through the TNT equivalency method, TNO multi-energy method and BST method is 10.5, 0.82 and 25.2, respectively. Referred to ASCE (2010), the ductility limitation of RC shear walls is 3. This wall design is not proper when checked with TNT equivalency and BST method. The rotation angle by three methods is 5.1°, 0.4°, 11.5°, respectively. The rotation angle of RC walls is different from 2° to 6° depending on the response level of a building. If the TNT equivalency method is used, the wall design is either passes or not. The TNO multi-energy method predicts it passed and BST method does it fails.

5) The PC panel connections are designed considering strength and dynamic increase factors. When the blast load is calculated based on TNT equivalency, TNO multi-energy and BST methods, the number of connection per meter is 3, 1 and 2, respectively. The total length of

wall is 26 m, so the total number of connections is 78, 26 and 52, respectively.

These comparative analyses show the differences of three empirical gas explosion methods. Through the first analysis, it is confirmed that the value of overpressure, duration or impulse is different depending on each method. The second analysis confirms the difference when methods are applied on real designs with the same scenario. Even results of design are not adjusted in all situations; they can be concrete examples confirming the differences of methods.

References

1. AISC (2011), "*Steel Construction Manual - Fourteenth Edition* (AISC 325-11)," American Institute of Steel Construction, Chicago, IL.

2. ASCE (American Society of Civil Engineering, 2010), "*Design of Blast Resistant Buildings in Petrochemical Facilities – Second Edition*," John Wiley & Sons, New York, NY.

3. AWS (2010), "*Structural Welding Code – Steel* (D1.1)," American Welding Society, Miami, FL.

4. Baker, Q. A., Tang, M. J., Scheier, E. A. and Silva, G. J. (1996), "Vapor Cloud Explosion Analysis," *Process Safety Progress*, V.15, No.2, 106-109.

5. Hjertager, B. H., Moen, I., Lee, J. H. S., Eckhoff, R. K., Fuhre, K. and Krest, O. (1981), "*The Influence of Obstacles on Flame Propagation and Pressure Development in a Large Vented Tube*," CM1 Report No. 803403-2, Chr. Michelsen Institute, Bergen, Norway.

6. Hjertager, B. H., Fuhm, K., Parker, S. and Bakke, J. R. (1982), "*Flame Acceleration of Propane-air in a Large-Scale Obstructed Tube*," CM1 Report No. 813403-5, Christian Michelsen Institute, Bergen, Norway.

7. Biggs, J. M. (1964), "*Introduction to Structural Dynamics*," McGraw-Hill Book Company, New York, NY.

8. Bjerketvedt, D., Bakke, J. R. and Van Wingerden, K. (1997), "*Gas Explosion Handbook*," Journals of Hazardous Materials, V.52, 1-150.

9. BSI (1997), "*Structural Use of Concrete Part 1: Code of Practice for Design and Construction* (BS 8110-1:1997)," British Standards Institution, London, UK.

10. Casal, J. (2007), "*Evaluation of the Effects and Consequences of Major Accidents in Industrial Plants*," Elsevier Science, Oxford, UK.

11. Cates, A. T. and Samuels, B. (1991), "A Simple Assessment Methodology for Vented Explosions," *Journal of Loss Prevention in the Process Industries*, V.4, 287-296.

12. CCPS (Center for Chemical Process, 1994), "*Guidelines for Evaluating the Characteristics of Vapor Cloud Explosions, Flash Fires, and BLEVEs*," American Institute of Chemical Engineers, New York, NY.

13. Commission for the Prevention of Disasters and Dutch Ministry of Social Affairs (1979), "*Methods for Calculation of the Physical Effects of the Escape of Dangerous Materials* (CPR14)," Directorate-General of Labour, Voorburg, The Netherlands.

14. Dusenberry, D. O. (2010), "*Handbook for Blast Resistant Design of Buildings*," Wiley, Hoboken, NJ.

15. Eggen, J. B. M. M. (1998), "*GAME: Development of Guidance for the Application of the Multi-Energy Method*," Health and Safety Executive Report No.202.

16. Harris, R. J. and Wickens, M. J. (1989), "Understanding Vapor Cloud Explosions—an Experimental Study." *55th Autumn Meeting of the Institution of Gas Engineers*, Kensington, UK.

17. Kinsella, K. G. (1993), "A Rapid Assessment Methodology for the Prediction of Vapor Cloud Explosion Overpressure," *International Conference and Exhibition on Safety, Health and Loss Prevention in the Oil*, Singapore, February.

18. Lea, C. J. and Ledin, H. S. (2002), "*A Review of the State-of-the-Art in Gas Explosion Modeling*," Health & Safety Laboratory (HSL), Buxton, UK.

19. Lee, S. and Lee, J (2012), "Building Design for Blast Resistance," *Review of Architecture and Building Science*, V.45, No.10, 58-62.

20. Lenoir, E. M. and Davenport, J. A. (1993), "A Survey of Vapor Cloud Explosions: Second Update," *Process Safety Progress*, V.12, No.1, 2-33.

21. Melani, L., Sochet, I., Rocourt, X., and Jallais, S. and Josas, F. (2009), "Review of Methods for Estimating the Overpressure and Impulse resulting from a Hydrogen Explosion in a Confined/Obstructed Volume," *International Conference of Hydrogen Safety*, Ajaccio, France.

22. Mercx, W. P. M. (1993), "*Modelling and Experimental Research into Gas Explosions: Overall Final Report on the MERGE Project*," Commission of the European Communities, Contract STEP-CT-011.

23. Mercx, W. P. M. and Van den Berg, A. C. (1997), "The Explosion Blast Prediction Model in the Revised CPR 14E (Yellow Book)," *Process Safety Progress*, V.16, No.3, 152-159

24. Mercx, W. P. M., Van den Berg, A. C. and Van Leeuwen, D. (1998), "*GAMES Application of Correlations to Quantify the Source Strength of Vapour Clouds Explosions in Realistic Situations*," Final report for the project GAMES, TNO Prins Maurits Laboratory, Norway.

25. Nasr, G. G. and Coner, N. E. (2014), "*Natural Gas Engineering and Safety Challenges: Downstream Process, Analysis, Utilization and Safety*," Springer, Switzerland.

26. OGP (International Association of Oil & Gas Producers, 2010) "*Risk Assessment Data Director – Major Accidents*", Report No. 434–17.

27. PCI (2004), "*PCI design handbook: Precast and Prestressed Concrete,*" Precase/Prestressed Concrete Institute, Chicago, IL.

28. Pierorazio, A. J., Thomas, J. K., Baker, Q. A. and Ketchum, D. E. (2004), "An Update to the Baker-Strehlow-Tang Vapor Cloud Explosion Prediction Methodology Flame Speed Table," *Process Safety Progress*, V.24, No.1, 59-65.

29. Puttock, J. S. (1995), "Fuel Gas Explosion Guidelines - the Congestion Assessment Method ," *2nd European Conference on Major Hazards On- and Off-shore*, Manchester, UK, September.

30. Puttock, J. S. (1999), "Improvements in Guidelines for Prediction of Vapour-cloud Explosions," *International Conference and Workshop on Modeling the Consequences of Accidental Releases of Hazardous Materials*, San Francisco, CA.

31. Ree, S., Kim, S. and Kang, T. H.-K. (2015), "Types of Explosions and Design Codes for Blast-resistant Structures," *Journal of the Korean Association for Shell and Spatial Structures* (*KASS*), V.15, No.3, 21-26 (in Korean).

32. Roberts, M. W. and Crowley, W. K. (2004), "Evaluation of flammability hazards in non-nuclear safety analysis," *EFCOG Safety Analysis Workshop*, San Francisco, CA, July.

33. Tang, M. J. and Baker, Q. A. (1999). "A New Set of Blast Curves from Vapor Cloud Explosion," *Process Safety Progress*, V.18, No.3, 235-240.

34. Thyer, A. M. (1997), "*Updates to VCE Modelling for Flammable Risk at: Part 1*," HSL Report No. RAS/97/04 - FS/97/01.

35. Turner, T. and Sari, A. (2012), “Vapor Cloud Explosion Prediction Methods – Comparison of TNO multi-energy (ME) and Baker-Strehlow-Tang (BST) Models in terms of Vulnerability of Structural Damage caused by an Explosion”, *ASCE Structures Congress 2012*, Chicago, IL.

36. UFC (United Facilities Criteria, 2008), “*Structures to Resist the Effects of Accidental Explosions* (UFC 3-340-02),” U.S. Army Corps of Engineers, Naval Facilities Engineering Command and Air Force Civil Engineer Support Agency.

37. Van den Berg, A. W. (1985), “The Multi-Energy Method – A Framework for Vapor Cloud Explosion Blast Prediction,” *Journal of Hazardous Materials*, V.12, 1-10.

38. Wiekema, B. J. (1980), “Vapour Cloud Explosion Model,” *Journal of Hazardous Materials*, V.3, 221-232

Appendix A : Comparative Analysis of Gas Explosion Methods

TNT equivalency method

Step 1. Compute the scaled distance.

$$Z = \frac{R}{W^{1/3}} = \frac{100 \text{ ft}}{\left(2204.6 \text{ lb}\right)^{1/3}} = 8 \qquad (2\text{-}1)$$

Step 2. Read off the overpressure, duration and impulse referred to **Figure 2-2**.

Spherical explosion :

P_{SO} = 10 psi (68.9 kPa), t_d = 0.029 sec and I_W = 628 (Pa·sec)

Hemispherical explosion :

P_{SO} = 13 psi (89.6 kPa), t_d = 0.029 sec and I_W = 897 (Pa·sec)

Same procedures are repeated as changing distance from the center.

TNO multi-energy method

Step 1. Compute the volume of vapor equivalent to the mass of TNT.

$$W_{TNT} = 0.16V_{cloud} \quad \leftrightarrow \quad 1000 \text{ kg} = 0.16V_{cloud}$$
$$V_{cloud} = 6,250 \text{ m}^3 \tag{2-4}$$

Step 2. Compute the combustion energy of vapor.

$$E_{comb.} = 3.5 \text{ MJ/m}^3 \times V_{cloud} = 3.5 \times 6,250 \text{ m}^3 = 21,875 \text{ MJ}$$
$$= 21.875 \times 10^9 \text{ J} \tag{2-5}$$

Step 3. Determine the scaled distance.

$$\overline{R} = \frac{R}{\left(E_{comb.}/P_a\right)^{1/3}} = \frac{30.28 \text{ m}}{\left(21.875 \times 10^9 \text{ J}/101,325 \text{ Pa}\right)^{1/3}} = 0.5 \tag{2-2}$$

Step 4. Compute overpressure at scaled distance 0.5 and determine the class number.

Class number ($\overline{R}$ = 0.5)	1	2	3	4	5	**6**	**7**	8	9	10
P_{SO} (kPa)	1.0	2.0	5.1	10.1	20.3	**50.7**	**94.2**	192.5	202.7	202.7

At this step, the corresponding class number is between 6 and 7. The analyzed class number will be 5, 6 and 7. The class number 5 is also used to show gap between strong and weak explosions.

Step 5. Read off the scaled overpressure and duration referred to **Figure 2-3**.

Variables	Class number		
	5	6	7
$\overline{P}_{SO}$	0.2	0.5	0.93
$\overline{t}_{+}$	0.71	0.39	0.3

Step 6. Compute the overpressure and duration.

$$P_{SO} = \overline{P_{SO}} \times P_0 = 0.2 \times 101,325 \text{ Pa} = 20,265 \text{ Pa} \tag{2-6}$$

$$t_d = \overline{t_d} \times \left(\frac{E_{comb.}}{P_0} \right)^{1/3} \times \frac{1}{a_0} = 0.71 \times \left(\frac{21.875 \times 10^9 \text{ J}}{101,325 \text{ Pa}} \right)^{1/3} \times \frac{1}{343 \text{ m/s}} \tag{2-7}$$
$$= 0.12$$

Step 7. Compute the impulse. Calculate the overpressure and duration.

$$I_W = \frac{P_{SO} \times t_d}{2} = \frac{20,265 \text{ Pa} \times 0.12 \text{ sec}}{2} = 1,258 \text{ Pa} \cdot \text{sec} \tag{2-8}$$

Same procedures are repeated as changing distance from the center.

BST method

Step 1. Determine the scaled distance in spherical and hemispherical explosions.

Spherical explosion :

$$\overline{R} = \frac{R}{\left(E_{comb.}/P_0\right)^{1/3}} = \frac{30.28\ \text{m}}{\left(21.875\times10^{9}\ \text{J}/101{,}325\ \text{Pa}\right)^{1/3}} = 0.5 \qquad (2\text{-}2)$$

Hemispherical explosion :

$$\overline{R} = \frac{R}{\left(\frac{E_{comb.}}{P_a}\right)^{1/3}} = \frac{30.28\ \text{m}}{\left(\frac{2\times21.875\times10^{9}\ \text{J}}{101{,}325\ \text{Pa}}\right)^{1/3}} = 0.4 \qquad (2\text{-}2)$$

Step 2. Compute overpressure at scaled distance and determine the Mach number.

M_w		0.2	0.35	**0.7**	**1**	1.4	2	3	4	5.2
P_{SO} (kPa)	Spherical ($\overline{R}$ = 0.5)	5.4	16.2	**50.7**	**83.1**	101.3	101.3	101.3	101.3	101.3
	Hemi-spherical ($\overline{R}$ = 0.4)	6.1	19.3	**58.8**	**101.3**	131.7	141.9	141.9	141.9	141.9

At this step, the corresponding Mach number is between 0.7 and 1. The analyzed Mach number will be 0.35, 0.7 and 1. The Mach number 0.35 is also used to show gap between strong and week explosions.

Step 3. Read off the scaled overpressure and the scaled impulse.

Type of exploson	Variables	Mach number		
		0.35	0.7	1.0
Spherical	$\bar{P}_{SO}$	0.16	0.5	0.82
	$\bar{I}_W$	0.05	0.06	0.06
Hemipshpherical	$\bar{P}_{SO}$	0.19	0.58	1
	$\bar{I}_W$	0.06	0.07	0.07

Step 4. Compute the overpressure and impulse.

Spherical explosion :

$$P_{SO} = \overline{P_{SO}} \times P_a = 0.16 \times 101,325 \text{ Pa} = 16,212 \text{ Pa} \tag{2-6}$$

$$\begin{aligned} I_W &= \overline{I_W} \times \left(\frac{E_{comb.}}{P_a} \right)^{1/3} \times \frac{P_a}{a_0} \\ &= 0.05 \times \left(\frac{2 \times 21.875 \times 10^9 \text{ J}}{101,325 \text{ Pa}} \right)^{1/3} \times \frac{1,013,225 \text{ Pa}}{343 \text{ m/s}} \\ &= 886 \text{ Pa} \cdot \text{sec} \end{aligned} \tag{2-9}$$

Hemispherical explosion :

$$P_{SO} = \overline{P_{SO}} \times P_a = 0.19 \times 101,325 \text{ Pa} = 19,252 \text{ Pa} \tag{2-6}$$

$$\begin{aligned} I_W &= \overline{I_W} \times \left(\frac{2 \times E_{comb.}}{P_a} \right)^{1/3} \times \frac{P_a}{a_0} \\ &= 0.06 \times \left(\frac{2 \times 21.875 \times 10^9 \text{ J}}{101,325 \text{ Pa}} \right)^{1/3} \times \frac{101,325 \text{ Pa}}{343 \text{ m/s}} \\ &= 1,340 \text{ Pa} \cdot \text{sec} \end{aligned} \tag{2-9}$$

Step 5. Compute the duration.

Spherical explosion :

$$I_W = \frac{P_{SO} \times t_d}{2} \rightarrow t_d = \frac{2 \times I_W}{P_{SO}}$$
$$t_d = \frac{2 \times 886 \text{ Pa} \cdot \text{sec}}{16,212 \text{ Pa}} = 0.11 \quad \text{(2-8)}$$

Hemispherical explosion :

$$t_d = \frac{2 \times 1,340 \text{ Pa} \cdot \text{sec}}{19,252 \text{ Pa}} = 0.14 \quad \text{(2-8)}$$

Same procedures are repeated as changing distance from the center.

Appendix B : Overpressure by Scenario

TNT equivalency method

Data

Combustion heat for propane gas = 46.3 MJ/kg

Mean specific heat for liquid propane = 2.41 kJ/kg/K

Latent heat for propane = 410 kJ/kg

Boiling point for propane = 231 K

Room temperature = 293 K

Combustion heat for TNT = 4.418 MJ/kg

Step 1. Compute flash fraction.

$$\begin{aligned} F &= 1 - \exp\left[\frac{-C_p \Delta T}{L}\right] \\ &= 1 - \exp\left[\frac{-(2.41 \text{ kJ/kg/K})(293 \text{ K} - 231 \text{ K})}{410 \text{ kJ/K}}\right] = 0.31 \end{aligned} \tag{4-1}$$

Step 2. Compute equivalent mass of TNT.

$$\begin{aligned} W_{TNT} &= \alpha_0 \frac{W_{fuel} H_{fuel}}{H_{TNT}} = \alpha_0 \frac{\left(2 \times F \times W_{propane}\right) H_{fuel}}{H_{TNT}} \\ &= 0.03 \frac{\left(2 \times 0.31 \times 25,000 \text{ kg}\right) \times 46.3 \text{ MJ/kg}}{4.418 \text{ MJ/kg}} \\ &= 4873 \text{ kg} \end{aligned} \tag{4-2}$$

Step 3. Compute the scaled distance.

$$\overline{R} = \frac{R}{W^{1/3}} = \frac{263 \text{ ft}}{(101743.13 \text{ lb})^{1/3}} = 12 \qquad (2\text{-}2)$$

Because the relation suggested by UFC (2008) is based on US unit, SI unit are converted; 80 m and 4873 kg are done to 263 ft and 101743.13 lb.

Step 4. Read off the overpressure and duration of the hemispherical explosion

Referred to **Figure 2-2 (b)**, overpressure and duration are 43.4 kPa and 0.065 sec.

TNO multi-energy method

Step 1. Compute the combustion heat of vapor cloud and scaled distance.

Combustion heat of propane gas :

$$E_{comb.} = 9{,}000 \text{ m}^3 \times 3.51 \text{ MJ/m}^3 = 31{,}500 \text{ MJ} \tag{2-5}$$

Scaled distance from center :

$$\overline{R} = \frac{R}{E_{comb.}} = \frac{80 \text{ m}}{\left(3.15 \times 10^{10} \text{ J}\right)^{1/3}} = 1.2 \tag{2-2}$$

Step 2. Read off the scaled overpressure and duration.

The class number is determined as 4 (**Table 2-2**). Referred to **Figure 2-3(a)** and **(c)**, the scaled overpressure and duration are 0.054 and 1.2, respectively.

Step 3. Compute the overpressure and duration.

$$P_{SO} = \overline{P_{SO}} \times P_a = 0.054 \times 101{,}325 \text{ Pa} = 5.47 \text{ kPa} \tag{2-6}$$

$$t_d = \overline{t_d} \times \left(\frac{E_{comb.}}{P_a}\right)^{1/3} \times \frac{1}{a_0} = 1.2 \times \left(\frac{3.15 \times 10^{10} \text{ J}}{101{,}325 \text{ Pa}}\right)^{1/3} \times \frac{1}{343 \text{ m/s}} \tag{2-7}$$
$$= 0.24$$

BST method

Step 1. Compute the combustion heat of vapor cloud and scaled distance.

Combustion heat propane gas :

$$E_{comb.} = 9{,}000\ \mathrm{m}^3 \times 3.51\ \mathrm{MJ/m}^3 = 31{,}500\ \mathrm{MJ} \tag{2-5}$$

Scaled distance from center :

$$\overline{R} = \frac{R}{\left(E_{comb.}/P_a\right)^{1/3}} = \frac{80\ \mathrm{m}}{\left(2 \times 3.15 \times 10^{10}\ \mathrm{J}/101{,}325\ \mathrm{Pa}\right)^{1/3}} = 0.94 \tag{2-2}$$

Because it is guessed as the hemispherical explosion, combustion energy is doubled.

Step 2. Read off and compute the scaled overpressure and impulse.

The Mach number is determined as 0.5 (**Table 2-4**). Because BST curves are suggested as the Mach number 0.35 and 0.7 (**Figure 2-5**). Scaled variables are calculated by interpolation.

Mach # 0.35 : $\overline{P}_{SO}$ = 0.1, $\overline{I}_W$ = 0.13

Mach # 0.7 : $\overline{P}_{SO}$ = 0.3, $\overline{I}_W$ = 0.2

Mach # 0.5 : $\overline{P}_{SO}$ = 0.19, $\overline{I}_W$ = 0.16

Step 3. Compute the overpressure and duration

$$P_{SO} = \overline{P_{SO}} \times P_a = 0.19 \times 101,325 \text{ Pa} = 19.3 \text{ kPa} \tag{2-6}$$

$$\begin{aligned} I_W &= \overline{I_W} \times \left(\frac{2 \times E_{comb.}}{P_a} \right)^{1/3} \times \frac{P_a}{a_0} \\ &= 0.16 \times \left(\frac{2 \times 3.15 \times 10^{10} \text{ J}}{101,325 \text{ Pa}} \right)^{1/3} \times \frac{101,325 \text{ Pa}}{343 \text{ m/s}} \\ &= 4034 \text{ Pa} \cdot \text{sec} \end{aligned} \tag{2-9}$$

$$\begin{aligned} I_W &= \frac{P_{SO} \times t_d}{2} \rightarrow t_d = \frac{2 \times I_W}{P_{SO}} \\ t_d &= \frac{2 \times 4034 \text{ Pa} \cdot \text{sec}}{19.3 \text{ kPa}} = 0.42 \end{aligned} \tag{2-8}$$

Appendix C : Equivalent Static Blast Load

Blast load

Step 1. Determine given conditions.

Check the peak overpressure, duration, height, width and length of building, and clearing distance.

Parameters	Method		
	TNT EM	TNO MEM	BST method
Peak overpressure (P_{SO})	43.4	5.37	18.76
Duration (t_d)	0.065	0.24	0.43
Height (B_H)	5		
Width (B_W)	Load case A = 3 / Load case B = 10		
Length (B_L)	Load case A = 10 / Load case B = 3		
Clearing distance (S)	Load case A = 1.5 / Load case B = 5		

Step 2. Compute blast parameters.

For convenience, dynamic pressure, shock front velocity and blast wave length are computed firstly.

Dynamic pressure, q_0 :

$$q_0 = 2.5{P_{SO}}^2 / \left(7P_0 + P_{SO}\right) \approx 0.0032{P_{SO}}^2 \tag{2-13}$$

Shock front velocity, U :

$$U \approx 345\left(1 + 0.0083P_{SO}\right)^{0.5} \tag{2-14}$$

Blast wave length, L_W :

$$L_W \approx U \times t_d \tag{2-15}$$

Step 3. Compute blast load and duration applied on the front wall.

The reflected coefficient, stagnation pressure, clearing time and impulse are computed like below:

Reflected coefficient, C_r :

$$C_r = P_r / P_{SO} \approx 2 + 0.0073 P_{SO} \tag{2-12}$$

Stagnation pressure, P_S :

$$P_S = P_{SO} + C_d q_0 \tag{2-16}$$

In front wall, the drag coefficient, C_d, is 1.0.

Clearing time, t_c :

$$t_c = 3S/U < t_d \tag{2-17}$$

Impulse, I_W :

$$I_W = 0.5\left(P_r - P_S\right) t_c + 0.5 P_S t_d \tag{2-18}$$

On front wall, the reflected overpressure and equivalent duration are applied.

Reflected overpressure, P_r :

$$P_r = C_r P_{SO} \approx \left(2 + 0.0073 P_{SO}\right) P_{SO} \tag{2-12}$$

Equivalent duration, t_e :

$$t_e = 2\, I_W \big/ P_r = \left(t_d - t_c\right) P_S \big/ P_r + t_c \tag{2-19}$$

Step 4. Compute blast load and duration applied on the side wall or roof.

On the side wall or roof, the side-on overpressure is applied, and total duration is computed. The reduction factor, C_e, is read referred to **Figure 2-11** with the length of unit element, L_1.

Side-on overpressure, P_a :

$$P_a = C_e P_{SO} + C_d q_0 \tag{2-20}$$

In the side walls or roof, the drag coefficient, C_d, is -0.4.

Rising time, t_r, and total duration, t_0 :

$$\text{Rising time : } t_r = L_1 \big/ U$$

$$\text{Total duration : } t_0 = t_r + t_d \tag{2-21}$$

Equivalent static blast load

Based on blast load and duration of each member, equivalent static load is calculated

Step 1. Compute properties of the unit member : gross moment of inertia, equivalent mass, stiffness and natural period.

Gross moment of inertia, I_{gross} :

$$I_{gross} = \frac{bh^3}{12}$$

Equivalent mass, M_{eq} :

$$M_{eq} = K_M M_{\text{unit member}}$$

The front wall is typically considered as the simply supported beam. The mass transformation factor, K_M, of the simple beam with distributed loading is 0.5.

Equivalent stiffness, K_{eq} :

$$K_{eq} = \frac{384EI}{L^3} \qquad (4\text{-}4)$$

The number, 384, is determined depending on boundary and loading conditions. Because this wall is designed based on the simply supported beam and distributed loading, 384 is applied.

Natural period, t_n :

$$t_n = \sqrt{M_{eq} / K_{eq}} \qquad (4\text{-}4)$$

Step 2. Compute ratio of duration and natural period, τ, and then ratio of maximum force and resistance, η.

The reflected overpressure and equivalent duration on the front wall are applied on maximum force, F_0, and natural period, t_n.

$$\tau = t_d / t_n$$

$$\eta = \frac{F_O}{R_m} = \frac{\sqrt{2\mu_d + 1}}{\pi(\tau)} + \frac{(2\mu_d - 1)(\tau)}{2\mu_d(\tau + 0.7)} \quad (4\text{-}3)$$

The maximum resistance, R_m, is dealt as equivalent static blast load.

국문초록

가스 폭발 실용모델 및 PC 패널의 방폭설계에 관한 비교분석 연구

가스 폭발 발생 위험이 큰 육상 플랜트 내에는 설비가 서로 가깝게 설치되기 때문에 중요 건물에는 모두 방폭설계를 적용하나 아직 플랜트 내 방폭설계에서는 별다른 기준이나 지침이 없다. 과거 BECTEL, BP 등과 같은 유명 석유회사에서는 TNT 당량을 이용한 폭발압력 산정 시방서를 보유하여 방폭설계에 적용하였다. 최근에는 주변 지리적 환경에 의해 폭발 결과가 달라지는 가스 폭발 특성을 고려하여 TNO 멀티에너지법이나 Baker-Strehlow-Tang(BST) 법 등의 실용모델을 이용한다. TNO 멀티에너지법은 class number, BST 법은 마하수에 따라 다른 결과가 예측되는데, 이 class number 및 마하수는 몇몇 해외 전문업체를 제외하고는 결정하기 힘든 값이다. 따라서 본 논문에서는 기존 TNT 당량에 의한 폭발압력이 TNO 멀티에너지법, BST 법에서 어떤 class number 및 마하수를 갖는지 조사하였다. 또한 초과압력, 폭발 지속 시간 및 충격량이 각 방법마다 조건에 따라 어떻게 달라지는지 비교하였다. 이에 더하여 시나리오 기반 설계를 수행할 경우 세가지 가스 폭발 예측방법에 따라 달라지는 설계결과의 차이를 비교 및 분석하였다.

연구 결과 기존 산업체에서 쓰이는 기준 중 가장 보수적인 기준(100 ft 혹은 30.5 m 에서 TNT 1 톤이 폭발한 경우)에 의한 폭발압력에 해당하는 class number 는 6 과 7 사이, 마하수의 경우 0.7 과 1.0 사이로 밝혀졌다. 비슷한 초과압력을 가질 때 TNT 당량법은 다른 방법에 비해 짧은 폭발 지속시간과 적은 충격량을 예측하는 것으로 나타났다. 또한 동일한 에너지를 갖는 폭발인 경우 거리에 따른 초과압력 변화량은 TNT 당량법이 가장 크게 나타났다. TNO 멀티에너지법과 BST 법은 class number 나 마하수가 높을수록 폭발 지속시간은 짧아지나 더 큰 충격량을 갖는 것으로 예측하는 것을 알 수 있었다.

한 가스 폭발 발생 시나리오를 기반으로 비교한 경우 TNT 당량법, BST 법, TNO 멀티에너지법 순으로 큰 초과압력을 예측하였으며, 200 mm 두께인 PC 패널의 방폭설계 역시 폭발 예측 방법에 따라 다른 결과를 나타내었다. 등가 단자유도 시스템을 이용하여 패널 양단 변형각을 계산할 경우, TNT 당량법은 5.1°, TNO 멀티에너지법은 0.4°, BST 법은 11.5°의 변형각을 발생시켰다. 건물 반응 정도에 따른 벽체 변형각 한계는 2° ~ 6° 이므로 가스 폭발 실용모델에 따른 부재 설계가 달라짐을 알 수 있다. 방폭설계를 적용한 PC 패널 연결부 요구 개수 역시 가스 폭발 실용모델에 따라 달랐으며 TNT 당량법, TNO 멀티에너지법, BST 법에 따른 필요 연결부의 개수 비율은 3:1:2 으로 나타났다. 본 연구를 통해 가스 폭발 실용모델에 따라 하중 뿐만 아니라 건물 방폭설계 결과에도 큰 차이가 나타남을 알 수 있었다. 아직 국내

다수 플랜트 업체에서는 방폭설계 시 기존 TNT 당량법을 이용한 설계법을 사용하나 최근 해외 플랜트 설계 발주가 증가함에 따라 TNO 멀티에너지법 및 BST 법에 대한 정보가 필요할 것으로 예상된다. 본 연구는 기존 TNT 당량법이 TNO 멀티에너지법 및 BST 법과 어떤 관계에 있는지, 각 방법에 따른 방폭설계가 어떻게 달라지는지 보여주는 연구로서 향후 육상 플랜트 실무자가 TNO 멀티에너지법 및 BST 법을 이용한 방폭 설계를 수행할 때 유용한 참고자료가 될 것으로 예상된다.

핵심용어: 가스 폭발, 가스 폭발 실용모델, 등가정적하중, 방폭설계, PC 패널

학번: 2014-20517